The use of geological 3D models to unravel Weichselian glacial history in Central Finnish Lapland and their application in groundwater flow modelling

ANNIKA ÅBERG

ACADEMIC DISSERTATION
To be presented, with the permission of the Faculty of Science of the University of Helsinki, for public examination in auditorium A111, Exactum, Kumpula Campus, on 19 August 2021, at 12 noon.

DEPARTMENT OF GEOSCIENCES AND GEOGRAPHY A93 / HELSINKI 2021

Cover figure: Annika Åberg
Back cover photo: Susanne Åberg

Author´s address: Annika Åberg
Department of Geosciences and Geography
P.O.Box 64
00014 University of Helsinki
Finland
annika.aberg@helsinki.fi

Supervised by: Docent Anu Kaakinen
Department of Geosciences and Geography
University of Helsinki

Docent Seija Kultti
Department of Geosciences and Geography
University of Helsinki

Professor Emeritus Veli-Pekka Salonen
Department of Geosciences and Geography
University of Helsinki

Reviewed by: Associate Professor Tiit Hang
Institute of Ecology and Earth Sciences
University of Tartu
Estonia

Professor Juha Pekka Lunkka
Oulu Mining School
University of Oulu
Finland

Opponent: Professor Emeritus Philip L. Gibbard
Scott Polar Research Institute
University of Cambridge
United Kingdom

ISSN 1798-7911
ISBN 978-951-51-6586-2 (pbk.)
ISBN 978-951-51-6587-9 (PDF)
http://ethesis.helsinki.fi

Unigrafia
Helsinki 2021

Åberg A. 2021. The use of geological 3D models to unravel Weichselian glacial history in Central Finnish Lapland and their application in groundwater flow modelling. Unigrafia. Helsinki. 53 pages, 4 tables and 14 figures.

Abstract

A proper risk assessment is part of mining projects from early stages to mine closure. Publicly companies present these assessments for example, in their Environmental Impact Assessment (EIA) reports. Potential risks related to water circulation can be investigated using groundwater flow modelling. In the present study, series of simple to more complex 3D geological models (GMs) were constructed from a Sakatti Ni-Cu-PGE deposit area in Sodankylä, northern Finnish Lapland to produce a numerical groundwater model. The 3D GMs were constructed utilizing data from outcrop investigations, various types of drillings and data obtained from non-destructive ground penetrating radar (GPR) soundings. In order to shed light on regional glacial history of central Finnish Lapland, outcrop studies, the existing till stratigraphy (GTK database) and LiDAR DEM imageries were used to investigate the sedimentary succession, interpret the depositional environments and reconstruct the Weichselian glacial flow patterns.

The results of this study indicate that complex and detailed geological models are beneficial, especially in areas with a high hydraulic gradient, multiple units with differing hydraulic conductivity, and altered upper bedrock zone with variable degrees of weathering. Furthermore, it is essential to identify low conductive units, such as interbedded fine-grained till units, as well as high conductivity units such as fractures and faults, since they affect the location of recharge and discharge areas in hydrostratigraphic flow models.

The 3D GMs constructed for the Sodankylä study area illustrate that altered bedrock, including fractured bedrock as well as grus- and clay-type weathered bedrock, is a prominent feature of the study area. The results of this study for example, indicate that fractured bedrock is more than 50 metres thick at the bend of the River Kitinen, while the grus-type weathered unit is on average 6 metres thick and the clay-type weathered unit 2.5 metres thick. Weak glacial erosion in the study area has enabled the preservation of Quaternary sediments spanning from pre-Weichselian, (most likely Saalian), to the Holocene. The thickness of the Quaternary deposits is variable, with an average thickness of approximately 8 metres. The Quaternary deposits consist of at least three separate till units and four interbedded sorted units. The Early Weichselian (MIS 5b) till unit is the most widespread and laterally continuous till unit in the area. The glacial lineations reflect pre-Late Weichselian glacial flow directions rather than rather than subglacially formed ice flow lineations formed during the Late Weichselian. During the Middle Weichselian stadial (MIS 4), the glacier flowed from N/NNE and had an overall weak impact on sedimentation, leaving sparse and thin remains of glacial till. The Late Weichselian glaciation (MIS 2) deposited a thin till cover, which was partly eroded by fluvial processes during the last deglaciation. Flow direction analysis of the till clast fabric suggests a northern location for the ice-divide zone during the Early and Middle Weichselian, and a more W/SW ice-divide position during the Late Weichselian. The optically stimulated lumines-

cence (OSL) age determination suggests ice-free areas in the vicinity of the River Kitinen valley already during the Bølling–Allerød warm period, indicating that ice had retreated from the area at that time patchy ice cover or rapid deglaciation.

Tiivistelmä (in Finnish)

Laaja riskinarvio on oleellinen osa kaivosprojektia sen eri vaiheissa, malminetsinnästä kaivoksen sulkemiseen. Kaivostoiminnan veden kiertoon ja pohjavesisysteemeihin liittyvät ympäristöriskit ovat merkittäviä. Näihin kohdistuvia riskejä voidaan tutkia pohjaveden virtausmallinnuksen avulla. Nämä pohjaveden virtausmallit pohjautuvat tutkimusalueelta tuotettuun 3D-geologiseen malliin.

Tässä väitöskirjatyössä tutkittiin jäätiköitymishistoriaa Sodankylässä sijaitsevan Sakatin Cu-Ni-PGE-esiintymän alueella sekä tuotettiin tutkimusalueelta 3D-geologinen malli numeeristen pohjaveden virtausmallien pohjaksi. Tutkimusaineisto koostui kattavasta maatutka-aineistosta, leikkaushavainnosta, OSL-ajoituksista sekä alueen LiDAR-korkeusmalleista. Lisäksi hyödynnettiin aiemmin julkaistua monipuolista kairaus- ja leikkaushavaintoaineistoa.

Yksinkertaisuusperiaatteen mukaisesti yksinkertaisin malli on todennäköisimmin toimiva havaintojen lisääntyessäkin. Tämä tutkimus kuitenkin osoitti, että monimutkaiset ja yksityiskohtaiset geologiset mallit ovat hyödyllisiä erityisesti alueilla, joilla on suuri hydraulinen gradientti, useita vedenjohtavuusominaisuuksiltaan vaihtelevia sedimenttiyksiköitä ja eriasteisesti rapautunutta sekä rakoillutta kalliota. Tämän lisäksi on olennaista tunnistaa matalan vedenjohtavuuden yksiköt kuten hienoainesmoreenit sekä vettä hyvin johtavat raot ja siirrokset, jotka vaikuttavat pohjaveden muodostumis- ja purkautumisalueiden sijainteihin hydrostratigrafisissa virtausmalleissa.

Sodankylän tutkimusalueelta tuotetut geologiset 3D-mallit osoittavat rapautuneen ja rakoilleen kallion ylimmän vyöhykkeen olevan merkittävä piirre tutkimusalueella. Rakoilleen kallion ylin vyöhyke yltää paksuimmillaan yli 50 metrin syvyyteen; grus-tyypin rapaumaa on keskimäärin 6 metriä ja savisen rapauman keskipaksuus on 2,5 metriä. Heikko jäätikkökulutus on mahdollistanut myöhäis-Veikseliä edeltävien kvartäärisedimenttien säilymisen, mahdollisesti jopa Saale-jäätiköitymisen ajalta. Kvartäärikerrostumien paksuus tutkimusalueella on keskimäärin 8 metriä. Alueen klastisista kvartäärikerrostumista voidaan erottaa kolme erillistä moreeniyksikköä ja neljä lajittuneen sedimentin yksikköä. Jatkuvin ja paksuin moreeniyksikkö on korreloitu Varhais-Veikseliin (MIS 5b). Keski-Veikselin (MIS 4) jäätiköitymiseen liitetty moreeni on puolestaan hyvin ohut ja pienialainen. Myöhäis-Veikselin jäätiköityminen (MIS 2) kerrosti melko ohuen moreenipeitteen, joka erodoitui osittain jokitoiminnan vaikutuksesta deglasiaation aikana.

Tutkimusalueen jäätikkösyntyisten muodostumien suuntaus on yhteneväinen moreenin suuntauslaskuista havaitun varhais-Veikselin jäätikön virtaussuunnan kanssa. Keski-Veikselin jäätiköitymisellä puolestaan vaikuttaa olleen heikko vaikutus alueen sedimentaatioon. Jäätikön virtaussuunta-analyysi moreenien suuntauslaskuista osoitti pohjoista–luoteista sijaintia jäänjakajalle varhais- tai keski-Veikselin aikana ja läntistä sijaintia myöhäis-Veikselin aikana. Eolisista sedimenteistä saatu OSL-ikämääritys viittaa alueen olleen ainakin osittain jäätön jo Bølling-Allerød -vaiheessa.

Acknowledgements

First of all, I am deeply grateful to Prof. Emer. Veli-Pekka Salonen, who invited me to join this project. I want to thank him for the guidance and inspiration for this work and for the encouragement I have received during these years. My greatest gratitude goes to my supervisors, Dr Anu Kaakinen and Dr Seija Kultti, who supported me during this doctoral study and provided advice that helped me to improve my thesis, especially during the second half of the project.

I am grateful to all my co-authors, Dr Kirsti Korkka-Niemi, Dr Emilia Koivisto, Dr Anne Rautio, Susanne Åberg and Kari Eskola, for their contributions and continuous support during various stages of the work. In particular, I am indebted to Dr Kirsti Korkka-Niemi for mentoring, motivation and for planning paper III, and to Dr Emilia Koivisto for her indispensable guidance with the GPR, which played a major part in my 3D model.

AA Sakatti Mining Oy made this study possible and is gratefully acknowledged. I am thankful for the fruitful cooperation, constant support and for sharing all the knowledge and data that helped me to improve the modelling part of my thesis. In particular, I want to thank Anne Rautio, Jukka Jokela, Pertti Lamberg, Janne Siikaluoma, Ulla Syrjälä and Joanna Kuntonen-van't Riet.

As for fieldwork, my gratitude goes to several former or extant students of the University of Helsinki. Jyri Laakso and Tatu Lahtinen helped during the field campaign in 2017, Markus Valkama's MSc thesis work provided useful information on the Kuusivaara outcrops, Mimmi Takalo and Harri Turtiainen provided GPR data across the Viiankiaapa mire and Rudi-Matti Suoknuuti participated in an extensive GPR acquisition campaign in 2019–2020 that was crucial to the construction of the GM2020 model.

This research was possible thanks to funding from the K.H. Renlund Foundation. The Doctoral Programme of Geosciences, University of Helsinki (GeoDoc), provided several travel grants, and the University of Helsinki provided a dissertation completion grant. The fieldwork was financed by several projects (Kuusivaara GPR, Sakatti Peat, Sakatti GPR), funded by AA Sakatti Mining Oy.

I am indebted to the pre-examiners of this PhD thesis, Prof. Tiit Hang and Prof. Juha Pekka Lunkka, whose suggestions and comments greatly improved this work.

I am grateful to Dr Jukka-Pekka Palmu and Dr Antti Ojala, who were inspiring teachers and mentors during my MSc thesis work and introduced me to the world of LiDAR maps. Special thanks to the members of the NordMin workshop in 2016, which advanced my thesis by providing inspiration for the reliability classification in Paper I.

I am thankful to Roy Siddall for the language revision of several papers and abstracts related to this work.

I extend my thanks to the colleagues at the Department of Geosciences and Geography over the years for the discussions and for creating a cosy workplace atmosphere, especially those who have shared the office with me during my doctoral project: Salla Eeva, Yurui Zhang, Tuomas Junna, Peter Howett and Juha Järvinen. Juha is also acknowledged for the high-resolution figures of the Kärväsniemi area, which helped me to virtually revisit my study area. I also wish to thank my former University of Helsinki colleague Juulia-Gabrielle Moreau for friendship and sharing many joyful moments. My gratitude also goes to Piritta Stark, who helped me during my GPR side-project by sharing the workload

with me during the final stages of my thesis. I am thankful to Veikko Peltonen for discussions on local bedrock and ice flow directions.

A special thank you to the people who helped me during my (un)fortunate adventures in Rome and Denver, Colorado: the couple in Colorado who helped me and my sister by giving food when we were in Dinosaur Ridge and the museum lady who gave us a lift back to our accommodation during a harsh storm, and a certain Roman gladiator who cheered us up in the preceding day in Rome during the IAH congress, when we had a shortage of cash.

Finally, my deepest gratitude goes to my parents and sisters. My parents have encouraged me in my geoscientific career, and my sister Susanne has been my closest colleague and collaborator and has shared the ups and downs during this project. My special thanks go to my relatives, who have supported me during these years and offered excellent dinners.

Contents

Abstract 5
Tiivistelmä (in Finnish) 7
Acknowledgements 8
List of original publications 12
Author's contribution 12
Abbreviations 13
List of Figures 14
1. Introduction 15
2. Study area and geological setting 16
3. Materials and methods 20
    3.1. GIS databases (Papers I, II & III) 20
    3.2. Sedimentological studies (Paper II) 22
    3.3. Ground penetrating radar (Papers I & III) 23
        3.3.1. GPR facies description and interpretation 23
    3.4. Three-dimensional (3D) modelling (Papers I, III & GM2020) 25
4. Results 27
    4.1. Results of Paper I 27
    4.2. Results of Paper II 29
    4.3. Results of Paper III 31
    4.4. The geological model GM2020 33
5. Discussion 33
    5.1. Three-dimensional (3D) geological models 33
        5.1.1. Input data for the 3D geological models 33
        5.1.2 Constructing 3D geological models 36
    5.2. Geological units, stratigraphy and glacial history of the study area 37
        5.2.1. Weathered and fractured bedrock 37
        5.2.2. Early Weichselian glaciation (KN Units 1–3, KU Units 1–2) 39
        5.2.3. Middle Weichselian glaciation (KN Unit 6) 40
        5.2.4. Late Weichselian (KN Unit 8, KU Unit 4) 42
        5.2.5. Deglacial and Holocene deposits (KN Unit 9, HI Unit 1, MU Unit 1, KU Units 5–6) 44
6. Conclusions 46
References 47

List of original publications

This thesis is based on the following publications:

I Åberg, A.K., Salonen, V.-P., Korkka-Niemi, K., Rautio, A., Koivisto, E. & Åberg, S.C. 2017. GIS-based 3D sedimentary model for visualizing complex glacial deposition in Kersilö, Finnish Lapland. Boreal Environment Research 22, 277–298.

II Åberg, A.K., Kultti, S., Kaakinen, A., Eskola, K.O., & Salonen, V.-P. 2020. Weichselian sedimentary record and ice-flow patterns in the Sodankylä area, central Finnish Lapland. Bulletin of the Geological Society of Finland 92, 77–98.

III Åberg, S.C., Åberg, A.K., & Korkka-Niemi, K. 2021. Three-dimensional hydrostratigraphy and groundwater flow models in complex Quaternary deposits and weathered/fractured bedrock: evaluating increasing model complexity. Hydrogeology Journal 29, 1041–1074.

The publications are referred to in the text by their roman numerals.

Author's contribution

I The study was designed by VPS. AÅ constructed the 3D model and prepared the manuscript with contributions from the other co-authors.

II The study was designed by VPS, AK and SK. All the authors participated in the fieldwork (2015). AÅ compiled and analysed the flow direction data and carried out the LiDAR analyses. AÅ was responsible for preparing the manuscript, while all the co-authors contributed and commented.

III The study was designed by all the authors. AÅ was responsible for the construction of the geological models. The manuscript was jointly written by all the authors.

Abbreviations

BOT	**B**ase **o**f **T**ill
ca.	***circa***
cf.	***confer***
CLGB	**C**entral **L**apland **G**reenstone **B**elt
DEM	**D**igital **E**levation **M**odel
EIA	**E**nvironmental **I**mpact **A**ssessment
ELY	**E**linkeino-, **l**iikenne-, ja **y**mpäristökeskus (Centre for Economic Development, Transport and the Environment)
e.g.	***exempli gratia***
et al.	***et alia***
GA	**G**older **A**ssociates
GI	**G**reenland **I**nterstadial
GS	**G**reenland **S**tadial
GM	**G**eological **m**odel
GPR	**G**round **P**enetrating **R**adar
GTK	**G**eologian **t**utkimus**k**eskus (Geological Survey of Finland)
HI	**Hi**etakangas
HSM	**H**ydro**s**tratigraphic **m**odel
i.e.	***id est***
KN	**K**ärväs**n**iemi
KU	**Ku**usivaara
LGM	**L**ast **G**lacial **M**aximum
LiDAR	**Li**ght **D**etection **a**nd **R**anging
m a.s.l.	**m**etres **a**bove **s**ea **l**evel
MIS	**M**arine **I**sotope **S**tage
MU	**Mu**ltaharju
OSL	**O**ptically **S**timulated **L**uminescence
SD	**S**tandard **d**eviation
SIS	**S**candinavian **I**ce **S**heet
WIP	**W**eathering **I**ndex of **P**arker

List of figures

Fig. 1. *Study area in central Finnish Lapland, page 17*
Fig. 2. *Geological setting of the study area, page 19*
Fig. 3. *Input data used in GM2020, page 24*
Fig. 4. *Examples of GPR facies and interfaces of this study with a 100-MHz antenna, page 26*
Fig. 5. *Simplified modelling workflow for the 3D model GM2020 with Leapfrog Geo and ArcMap software, page 28*
Fig. 6. *Composite stratigraphy of the Sodankylä area and comparison with the Northern European stratigraphy and global benthic $\delta^{18}O$ data, page 30*
Fig. 7. *Results of flow direction analysis within the LiDAR inspection areas: Kittilä, Sodankylä and Salla, page 32*
Fig. 8. *"Exploded view" of the 3D geological model (GM2020) in Sodankylä, central Finnish Lapland, page 34*
Fig. 9. *Four versions of the geological model in the Sakatti area, page 36*
Fig. 10. *Distribution of the 3D modelled units in GM2020, page 38*
Fig. 11. *Fence section of GM2020 along GPR profile 112, page 43*
Fig. 12. *Geological cross-section through KN-1 and KN-2, page 43*
Fig. 13. *Glacial lakes and estimated glacier limits within the study area, page 44*
Fig. 14. *Geological cross-section through Pahanlaaksonmaa and Sahankangas, page 46*

1. Introduction

Relict landscapes, including tors, rounded inselbergs, and the weathering crust in the area extending from northern Sweden to northern Finland shows clear evidence of weak glacial erosion prior to and during the Pleistocene glaciations; the deep weathered crust dates back at least to Paleogene and Neogene (Hirvas, 1991; Ebert *et al*., 2015). Studies on glacial history of the area dates back to early 1900s and have continued ever since to reveal the Quaternary stratigraphy, glacial history and more recently the dynamic history of the Scandinavian Ice Sheet during the Weichselian and also during the previous glacial stages (Paper II; Tanner, 1915; Kujansuu, 1967; Hirvas, 1991; Olsen *et al*., 1996; Helmens *et al*., 2000; Hättestrand & Robertsson, 2010; Helmens, 2014; Salonen *et al*., 2014b; Lunkka *et al*., 2015; Howett *et al*., 2015; Helmens, *et al*., 2018). As early as in the 1930s, Tanner (1930) concluded on the basis of sedimentological succession and till-covered glaciofluvial deposits that instead of one permanent ice cover, Finland was ice-free at least once during the last ice age. Later, the development of the optically stimulated luminescence (OSL) method enabled the dating of quartz-bearing sorted deposits, which suggested the existence of several stadials and interstadials during the Weichselian (*e.g*. Hättestrand & Robertsson, 2010; Salonen *et al*., 2014b; Lunkka *et al*., 2015).

The relative weak glacial erosion area coincides with the Central Lapland Greenstone Belt (CLGB) that has been the subject of intensive investigation during the last decades as a consequence of the ore potential of (Eilu, 2012). Furthermore, the sustainable use of raw materials currently has a major role in the mineral strategy of Finland, including the reduction and prevention of environmental hazards (Mineraalistrategia, http://projects.gtk.fi/mineraalistrategia/index.html [in Finnsh]). At the same time, the increasing demand for raw materials has led to the pressure to use raw materials that lie in/under natural conservation areas, such as the Sakatti Cu–Ni–PGE deposit (Brownscombe *et al*., 2015), or close to conservation areas, such as the Hannukainen Fe–Cu–Au deposit (Niiranen *et al*., 2007). Typically, the potential environmental risks are related to the hydrology and hydrogeology of planned mining sites (*e.g*. Gray, 1997; Kauppi *et al*., 2013; Salonen *et al*., 2014a; Åberg *et al*., 2019).

General concern of sustainable practices in mining operations has raised interest to understand the water cycle of possible mining sites prior to the start of mining operations (Salonen *et al*., 2014a; Rautio *et al*., 2018; Åberg *et al*., 2019). The water cycle can be assessed using a numerical groundwater flow model. In order to generate a reliable groundwater model requires understanding of the subsurface structures, which can be visualized with a 3D geological model (GM). The input data for a 3D GM can vary depending on the study site, typically consisting of data acquired from drillings, outcrop surveys and geophysical data. The area of interest may lie in an area where a dense drilling network is difficult to carry out. These type of areas are, for example, located adjacent to conservation areas or in an area where sediment overburden above the bedrock is thick. However, the lack of drilling data, for example, in the areas of thick Quaternary deposits can be compensated using non-destructive methods, such as ground penetrating radar (GPR) survey to obtain data for GM models.

Sakatti Ni-Cu-PGE deposit area in Sodankylä, northern Finnish Lapland within the CLGB is a target area for an intensive exploration program. At the same time, there is an urgent need for a better estimate of possible environmental hazards caused by mining activities (Salonen

et al., 2014a; Rautio *et al*., 2018; Åberg *et al*., 2019). This is true especially in the areas covered by nature conservations programs (Natura 2000) as is the case in the study area discussed here. This study produces information for the Environmental Impact Assessment (EIA) process and decision making based on a set of geological and hydrogeological baseline data from Sakatti exploration area along the River Kitinen. The main objectives of this study are:

- To create a 3D model of Quaternary sediments by combining all existing observations with new drilling data, targeted GPR soundings and LiDAR-DEM imageries
- To reconstruct the Weichselian glacial history and sediment succession in Sodankylä area and to interpret the local depositional environments
- To synthesize the Weichselian ice-flow patterns in Central Finnish Lapland and to compare the flow directions derived from the streamlined features with those from the till clast fabric analyses
- To evaluate the efficiency of increasing GM complexity to groundwater flow model performance in hydrostratigraphically heterogenic environment

A detailed 3D GM was constructed with the 3D modelling software Leapfrog Geo (Seequent Ltd.) for the area hosting the Sakatti Cu-Ni-PGE deposit (Paper I). The 3D GM presented in this study formed the basis for a groundwater flow model (Paper III and Åberg S. *et al*., *in prep.*) and sheds light on the complex glacial history of the Sodankylä area. The input data for the 3D GM consisted of outcrop studies, drillings (diamond drilling, auger drilling, vibration drilling), "Targeting till geochemistry" dataset and non-destructive GPR data acquisition. For a more regional view of the glacial history of central Finnish Lapland, outcrop studies, existing till stratigraphy (GTK database) and LiDAR-DEM imageries were used to investigate the sedimentary succession, interpret the depositional environments and reconstruct the glacial flow patterns during the Weichselian (Paper II).

2. Study area and geological setting

The study area is located in Sodankylä in northern Finnish Lapland, along the River Kitinen (Fig. 1). The topography is undulating, and consist of mire-covered river valleys and inselbergs that rise above the flat topography. The highest inselbergs reach altitudes of 410 metres above sea level (m a.s.l.), rising 10–160 metres from the flat-lying area. The altitude of the river valleys varies from 158 to 220 m a.s.l. The four largest rivers that cross the study area are the River Jeesiöjoki crossing the Kittilä and Sodankylä area, the River Kitinen and the River Sattanen in the Sodankylä area and the River Luiro in the Salla area (Fig. 1). Peatlands are abundant at lower altitudes. The two largest peat land areas are the Viiankiaapa mire on the eastern side and the Vanttioaapa mire on the western side of the River Kitinen (Fig. 1). The southern part of the study area is covered by smaller peat lands, including Eliasaapa south to Kuusivaara and Kotiaapa in the SW corner of the study area. The Sakatti Ni-Cu-PGE deposit was discovered beneath the Viiankiaapa mire (Brownscombe *et al*., 2015), which has been a nature conservation area since 1988 and belongs to the European Union's Natura 2000 network (Hjelt & Pääkkö, 2006). The mire covers an area of 5385 ha (Lappalainen, 2004). According to field studies conducted in 1965, the peat deposit is 2.3 metres thick on average, and 5.7 metres thick in its deepest part (GTK, unpublished data). Over the half of the mire consists of mesotrophic patterned fens and one quarter is composed of tree-covered

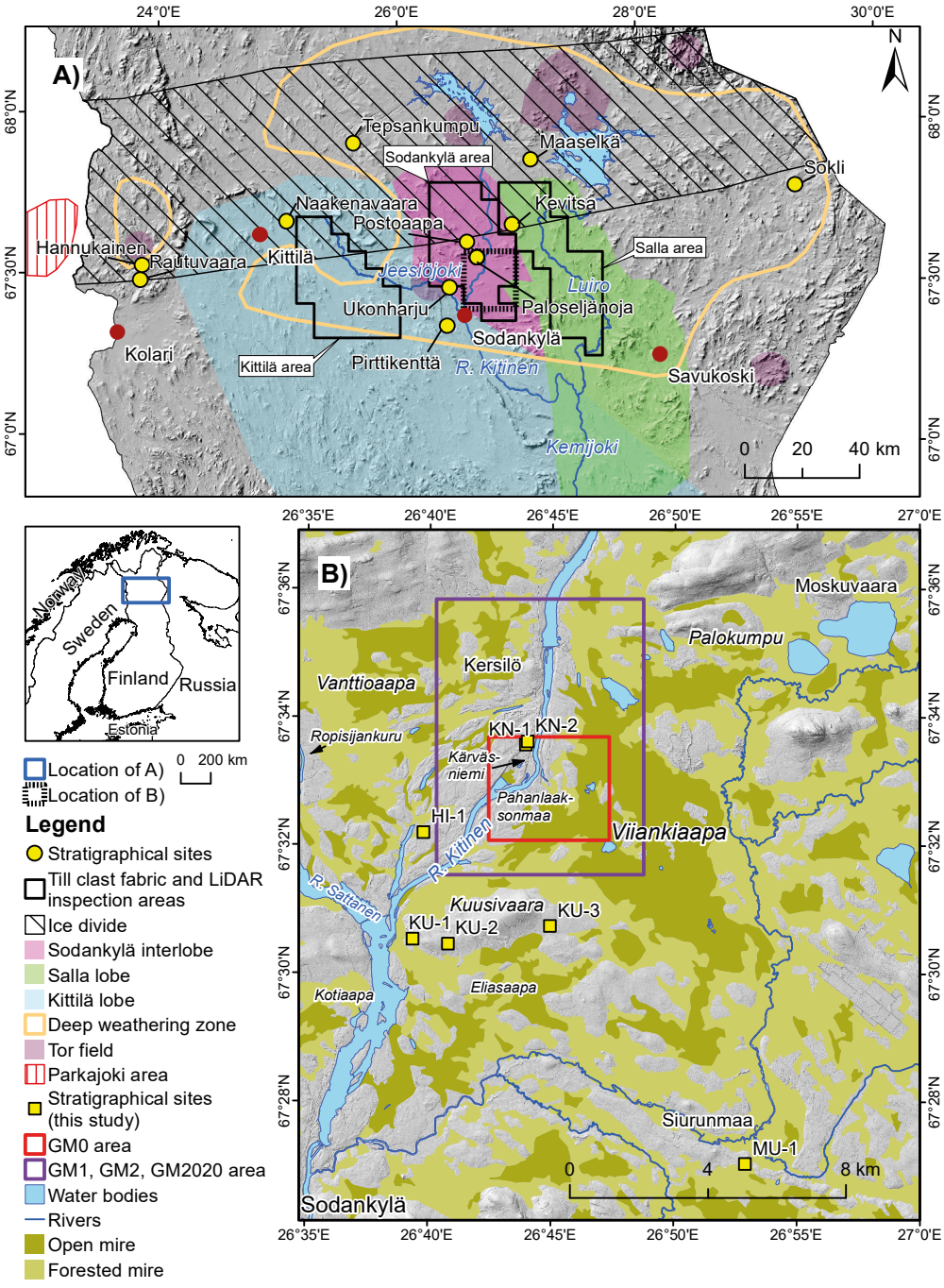

Figure 1. Study area in central Finnish Lapland. A) Location of areas for till clast fabric and glacial lineation analyses (LiDAR inspection). The Kittilä, Sodankylä and Salla areas in central Finnish Lapland and corresponding ice lobe and interlobe areas (Paper II). B) The studied sections and the 3D modelled areas, GM0–GM4. Administrative borders of Norway, Russia and Sweden: www.gadm.org (visited 4/2017). Basemap elements are modified after National Land Survey of Finland. Deep weathering zone, tor field and Parkajoki area are modified after Ebert *et al.* (2015). Ice divide is modified after Johansson *et al.* (2011). Water bodies in A and rivers are modified after Finnish Environment Institute, 2014.

pine and spruce mires (Hjelt & Pääkkö, 2006). Several protected moss species, such as *Hamatocaulis vernicosus*, *Hamatocaulis lapponicus*, *Meesia longiseta* (Ramboll, 2020), *Palustriella falcata*, *Palustriella decipiens* and *Catoscopium nigritum*, as well as endangered vascular plants such as *Saxifraga hirculus* and *Carex heleonastes* grow in the Viiankiaapa mire (Hjelt & Pääkkö, 2006).

The bedrock of the study area belongs to the Palaeoproterozoic CLGB (Hanski *et al*., 2001; Hanski & Huhma, 2005; Niiranen *et al*., 2015). The CLGB overlies Archean basement rocks and is confined by the Central Lapland Granitoid Complex (Hanski *et al*., 2001; Hanski & Huhma, 2005; Niiranen *et al*., 2015) (Fig. 2A). In the study area, the CLGB consists of gabbros, mafic volcanic rocks and metamorphosed sedimentary rocks (Tyrväinen, 1980, 1983; GTK, 2018). The most prominent faults in the Sodankylä area follow the lithological contacts striking mostly W–E (Fig. 2A, GM2020 area). The main W–E-oriented fault zones are cut by NW–SE-oriented fractures.

The solid crystalline bedrock is covered by altered bedrock including fractured bedrock as well as grus- and clay-type weathered bedrock (saprolite), which is an abundant feature in central Lapland (Hirvas, 1991; Hall *et al*., 2015). Bedrock alteration is gradual where fractures (*i.e*. faults and joints), their spacing and chemical weathering stage increases upward to the bedrock surface. The thickness and type of chemical weathering varies within the study area (Rask & Lintinen, 2001; Hall *et al*., 2015) as well as the proportion between the chemical and physical weathering. In general, the chemically weathered saprolite is thicker in the greenstone and shear zone areas, where it can be over 20 metres thick (Hall *et al*., 2015). Tripartite weathering consists of chemically altered clay-rich kaolinitic weathered zone underlain first by a sand-like grus weathering zone and a more compact saprock occurs at the base. Bipartite weathering consists of less chemically altered grus and saprock. Of these, bipartite weathering is more widespread in the peneplain area of Sodankylä (Lestinen, 1980). An exceptional thick clay weathering crust (20–50 m) has been observed in Siurunmaa in the Sodankylä area (Hall *et al*., 2015) (Fig. 1).

Central Finnish Lapland lies in the central part of an area affected by weak glacial erosion (Hirvas, 1991; Ebert *et al*., 2015). The Scandinavian Ice Sheet (SIS) has covered the area several times during the Pleistocene (*e.g*. Hirvas, 1991; Aalto *et al*., 1992; Svendsen *et al*., 2004; Batchelor *et al*., 2019) and as a consequence, the area is covered by tills deposited during multiple glacial events. The till covered-landscape is dissected by glaciofluvial, fluvial and aeolian deposits, which are abundant in river valleys. Peat accumulation in the flat-lying peneplains started after the last deglaciation (Johansson & Kujansuu, 2005) *ca*. 10 ka BP (Suonperä, 2016).

Based on subglacial lineation patterns deduced from the LiDAR-DEM imageries, Putkinen *et al*. (2017) recognized two different ice-stream lobes in central Finnish Lapland; the Kuusamo ice-stream lobe to the west of Sodankylä and the Salla ice-stream lobe to the east of the Sodankylä region (Fig. 1A). The northernmost branch of the Kuusamo ice-stream lobe is located in the Kittilä area, and it is, therefore, referred as the Kittilä lobe in this study. The Sodankylä region is almost void of subglacial lineation forms and therefore, it is referred here as the Sodankylä interlobate area. The analysis of the LiDAR-DEM imageries on glacial landforms shows that, glacial lineations, including drumlins and drumlinoids, are common in the Salla and Kittilä areas, whereas in the Sodankylä area, glacial lineations are rare. The LiDAR-DEM imageries also reveals hummocky moraine fields in

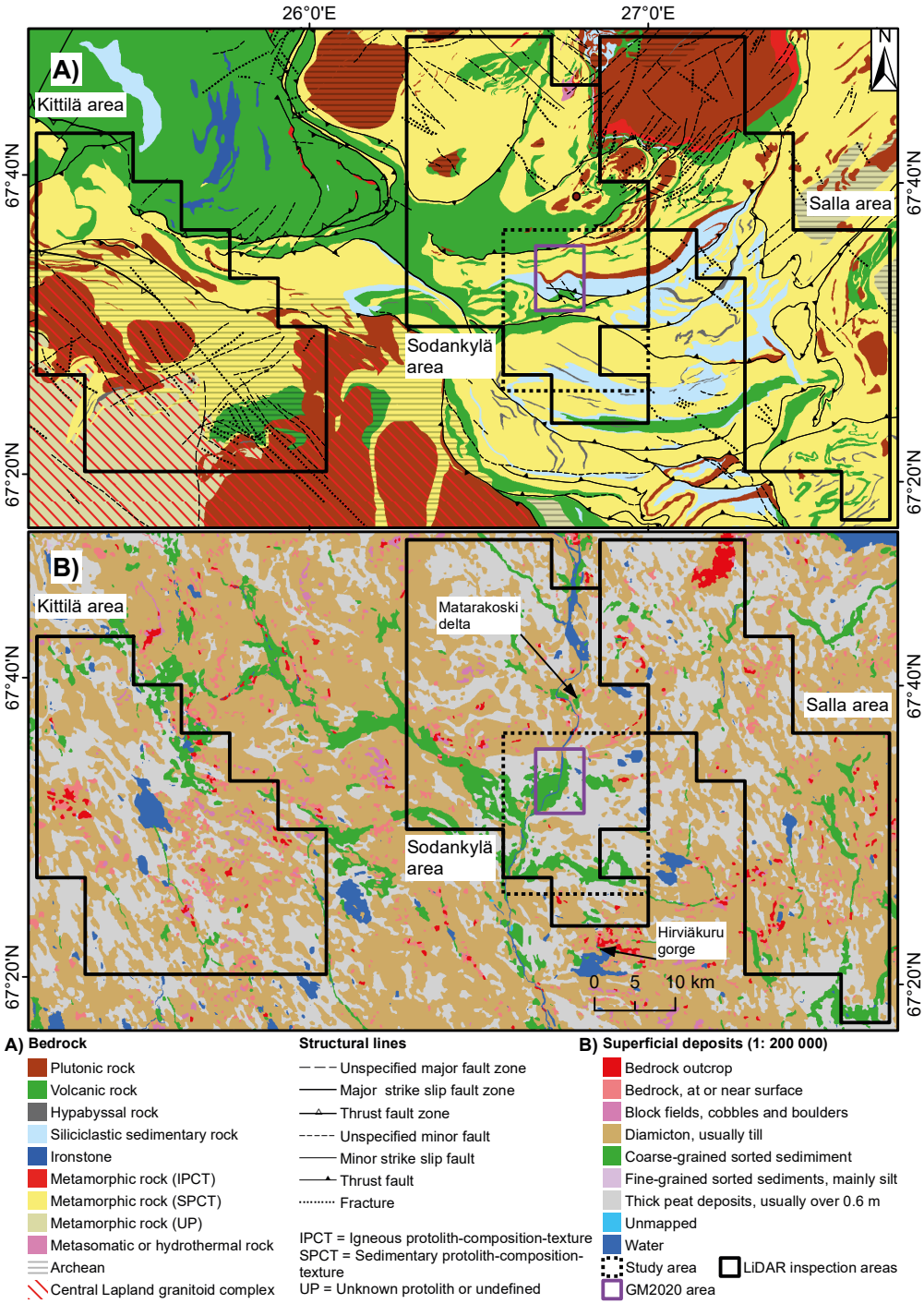

Figure 2. Geological setting of the study area. For the location, see Fig. 1A. A) Bedrock map of the study area. B) Quaternary deposits of the study area. Bedrock of Finland (scale free), structural lines (scale free), and superficial deposits 1: 200 000: © Geological Survey of Finland, used with permission.

southern parts of the Sodankylä and Salla areas.

Glaciofluvial sorted deposits in the study area include eskers and outwash plains. The latter are often located upstream of converging river channels and have been dissected by recent river channels. Outwash plains are most prominent in the Sodankylä area along the rivers Kitinen and Sattanen, outwash plains also exists in the Kittilä and Salla areas along the rivers Jeesiöjoki and Luiro. Eskers are common in central Finnish Lapland, but they are rare in the Sodankylä interlobate area. In central Finnish Lapland there are two, often till-covered esker systems. One system, where the esker ridges, composed of coarse material, are oriented NW–SE and another esker system where the esker ridges are oriented N–S (Johansson, 1995). Of these two esker systems, the one oriented NW–SE is considered to be an older system compared to the N–S oriented system (Sutinen, 1992; Johansson, 1995). Moreover, in the eastern part of the Salla area is an esker system consisting of discontinuous ridges that have been interpreted to represent the youngest meltwater system, indicating glacial retreat towards the NW (Johansson, 1995; Johansson & Kujansuu, 2005). Previous studies have indicated that till-covered glaciofluvial interstadial deposits are common within the study area, especially in Sodankylä (Sarala *et al*., 2015). OSL dating results of till-covered glaciofluvial deposits suggest that they formed during during one of the Early Weichselian interstadials (Sarala *et al*., 2015).

Aeolian deposits exist in the River Kitinen valley at Sodankylä, where dune fields have deposited on the flat-lying areas (Räisänen, 2014; Sarala *et al*., 2015). According to the LiDAR-DEM interpretation of the aeolian landforms, the prevailing wind direction has been from the west during their formation. Similarly, in the Kittilä and Salla areas, aeolian deposits are located in river valleys.

Lacustrine deposits in the study area were laid down to the Moskujärvi Ice Lake, which occupied the area at the transition from the Weichselian to the Holocene and during the Ancylus Lake phase of the Baltic Sea (Johansson & Kujansuu, 2005). The lacustrine Moskujärvi Ice Lake sediments lie on the eastern side of the study area below 207 m a.s.l., while lacustrine sediments deposited into the Ancylus Lake occur at lower elevations than 186 m a.s.l. (Johansson & Kujansuu, 2005), mainly underlying the Viiankiaapa mire (Pääkkö, 2004; Suonperä, 2016) and other low-lying mire areas.

Peat is the most abundant organic sediment in the study area. There are also few sites where organic sediments (such as gyttja) have been found beneath till (*cf*. Hirvas, 1991). These sites are located in the mire areas *e.g*. Viiankiaapa, Postoaapa and Paloseljänoja, and considered to have been deposited during the Eem interglacial (Hirvas, 1991) (Fig. 1).

3. Materials and methods

3.1. GIS databases (Papers I, II & III)

All available information on Quaternary deposits, the bedrock surface and weathered bedrock was collected from the River Kitinen valley (X: 482000–500000, Y: 7480000–7500000; EUREF_FIN_TM35FIN; E: 26° 34,779'–27° 0,000', N: 67° 26,135'–67° 36,932'; WGS84) for 3D modelling (study area indicated in Fig. 2, Table 1). The information sources included public databases: the Hakku service of the Geological Survey of Finland (available at https://hakku.gtk.fi/) and Avoin tieto of Finnish Environmental Institute (SYKE, http://www.syke.fi/fi-FI/Avoin_tieto/Ymparistotietojarjestelmat [in Finnish]). Additional GIS databases were compiled from the literature, as well as from unpub-

Table 1. Previously published data used in this study.

Database name	Observations	Data points[1]	Profiles	Source	Paper I	Paper II	Paper III
Auger drillings	22	60	22	Leskelä, 1971	x		x
Auger drillings	12	20	12	Salminen, 1972	x		x
Bedrock observations	415	415	-	GTK Hakku			x
BOT observations 2005–2012	2181	2263	-	AA Sakatti mining Oy, unpublished	x		x
BOT observations 2013–2014	4449	4449	-	AA Sakatti mining Oy, unpublished			x
Detailed till geochemistry	809	1026	87	GTK Hakku			x
Eskers	168	-	-	Superficial deposits database, GTK Hakku		x	
Eskers	8	-	-	Paper II		x	
Glacial lineations	435	-	-	Superficial deposits database, GTK Hakku		x	
Glacial lineations	130	-	-	Paper II		x	
Groundwater wells ELY	10	47	10	ELY centre, unpublished			x
Groundwater wells GA	24	24	24	Golder Associates, 2012, unpublished	x		x
Groundwater wells Hertta	38	38	1	Avoin tieto, Hertta[2]	x		
Groundwater wells Moskuvaara	12	27	12	Lapin ELY-keskus	x		
Groundwater wells Sakatti	13	143	13	AA Sakatti mining Oy, unpublished			x
National drill core archive 1979–1996[3]	36	36	-	GTK Hakku	x		
Overburden thickness 2006–2016[3]	161	161	-	AA Sakatti mining Oy, unpublished	x		x
Overburden thickness 2016–2019[3]	111	111	-	AA Sakatti mining Oy, unpublished			x
Peat investigations 1965	311	311	-	Lappalainen, 1970	x		x
Peat investigations 1975	91	91	-	Lappalainen & Pajunen, 1980	x		x
Peat thickness HU	6	6	6	Paper III			x
Peat thickness Sakatti	12	12	-	AA Sakatti mining Oy, unpublished			x
Sections 2015	4	18[4]	9	Paper I, Paper II	x	x	x
Sections Kuusivaara	3	10[4]	3	Paper II		x	
Sections Palokumpu	2	2[4]	2	Paper I	x		
Stratigraphical sites	2	2	2	Hirvas, 1991	x		x
Striations	18	-	-	Striations , GTK Hakku		x	
Striations	3	-	-	Salmi, 1965		x	
Striations	1	-	-	Tanner, 1915		x	
Superficial deposits database[5]	104	224	103	GTK Hakku			x
“Targeting till geochemistry” database	1936	3906	608	Gustavsson *et al.*, 1979	x		x
Test pits GTK	12	12	12	Hirvas *et al.*, 1977	x		x

Till fabrics	110	-	-	Superficial deposits database, GTK Hakku		x	
Till fabrics	2	-	-	Hirvas *et al*., 1994		x	
Till fabrics	1	-	-	GTK, unpublished		x	
Till fabrics	1	-	-	Hirvas, 1991		x	
Vibration drillings 1986–87	20	39	20	Lapin vesi- ja ympäristö-piiri, 1988, unpublished	x		x
Vibration drillings 1998	49	152	49	Lapin ympäristökeskus, 1998, unpublished	x		x

[1]Total sample (data point) count.

[2]http://www.syke.fi/fi-FI/Avoin_tieto/Ymparistotietojarjestelmat [in Finnish].

[3]Diamond drillings

[4]Unit count.

[5]Vibration drillings

lished data of AA Sakatti Mining Oy, the Centres for Economic Development, Transport and the Environment (ELY Centre) and the Geological Survey of Finland (Table 1). In addition to 3D modelling, glacier flow direction analysis was carried out for the Kittilä, Sodankylä and Salla areas, each covering an area of 1050 km² (Figs. 1 and 2). The features that depict the glacier movement directions (glacial lineations, eskers, striations and till clast fabrics) were compiled from the Hakku service and previous studies (Table 1). In addition, 130 new subglacial lineation forms were mapped from a 2-metre-horizontal-resolution LiDAR DEM. A more detailed description of the flow direction analysis is presented in Paper II.

3.2. Sedimentological studies (Paper II)

A total amount of seven excavated exposures at Kärväsniemi, Hietakangas, Kuusivaara and Multaharju were studied during the fieldwork campaigns in 2015 and 2017 (Fig. 1 and Table 2). The outcrops were studied for their lithofacies, unit boundaries and dimensions, as well as deformation structures. The lithofacies classification used was modified from Eyles *et al*. (1983). Six till clast fabrics and 22 granulometric analyses were carried out from sediment units in exposures. The till fabrics were calculated on average from 50 clasts within one square metre area. The fabric measurements were made with five-degree accuracy of elongate clasts with an *a*-axis minimum length of 0.5 cm and *a*/*b* axes ratio of ≥1.5. Granulometric analyses were conducted with gravitational methods based on the instructions of Tie-ja vesirakentamishallitus (1973). Gravimetric methods included dry sieving, wet sieving and hydrometer analysis.

Optically stimulated luminescence (OSL) is a dating method suitable for quartz or K-felspar bearing minerals. Seven samples for optical dating were collected from the sites using Ø 5-cm PVC tubes driven directly into freshly cleaned pit faces. The sampled units represented well-sorted medium to fine sands in shallow channel fills, aeolian dunes and palaeosols (Table 2 in Paper II). *In-situ* gamma dose measurements, including cosmic radiation, for the OSL age determinations were recorded using a portable ICx-Identifinder gamma spectrometer with a Ø1.4”×2” NaI(TI) detector.

OSL measurements and sample preparation were performed in the Laboratory of Chronology, Finnish Museum of Natural History, University of Helsinki. The beta dose rate was de-

termined in the laboratory using a Risø GM-25-5 beta multicounter (Bøtter-Jensen & Mejdahl, 1988). The effects of the water content on the dose rates were calculated according to Aitken (1985). Water contents of Wsample = Wsoil = 0.2 (saturation water content 20%) were used in the analysis since the sampled units had been below the areal groundwater table most of their time after the deposition. The OSL measurements were implemented from quartz using an upgraded Risø TL-DA-12 reader (Bøtter-Jensen & Duller, 1992; Bøtter-Jensen *et al*., 1999). The single aliquot regeneration (SAR) protocol (Murray & Wintle, 2000) was used as a base for the measurement procedure. Further details of the OSL procedure are described in Paper II.

3.3. Ground penetrating radar (Papers I & III)

The GPR data was collected using 30, 50, 100 and 250 MHz antennae from the GPR survey lines covering 230 km in total (Fig. 3). The apparatus used was MÅLA Ramac ProEx GPR. The altitude correction of GPR profiles was derived from the LiDAR-DEM imageries. The GPR profiles were processed with Reflexw software (versions 7–9, Sandmeier: https://www.sandmeier-geo.de/reflexw.html). A standard procedure for the GPR processing was developed, including amplitude, time-zero and topographic corrections, various filtering steps and time-to-depth corrections. A basic velocity of 0.1 m ns^{-1} was used for the majority of the GPR profiles (Neal, 2004) for the electromagnetic waves, the velocity being verified with drill-hole data along the GPR. If the GPR profile included peat, a velocity correction corresponding to the peat thickness was made with a velocity of 0.04 m ns^{-1} (Neal, 2004). Additional velocity corrections were made for the flood plain sediment area along the River Kitinen (fine sand in the surficial deposit map of GTK), where a velocity of 0.07 m ns^{-1} (Neal, 2004) was applied. In addition, 8 km of processed GPR profiles by GTK (Lapin POSKI, Kupila *et al*., 2020) and 2 km of processed GPR profiles by GEOFCON (unpublished data) were utilized in this study.

3.3.1. GPR facies description and interpretation

After processing of the GPR data, the GPR profiles were interpreted and the interfaces of the subsurface were picked with Reflexw. The 100-MHz profiles were principally used for the interpretation due to their higher resolution and ability to detect thinner units. The 50-MHz and 30-MHz profiles supported the interpretation of the lower parts of subsurface due to their greater penetration depth. The first step in the interpretation was to identify the sharp interfaces, such as the groundwater table, bedrock surface, the basal contact of the peat and other sharp bound-

Table 2. The locations and the sediment thickness of the exposures studied in the River Kitinen valley, Sodankylä. The OSL-sampled and till clast fabric analysis sites are also indicated.

Name, site	Coordinates	Top (m a.s.l.)	Thickness (m)	OSL	Till clast fabric
KN-1, Kärväsniemi	67° 33.569' N, 26° 43.915' E	186.6	5.6	x	x
KN-2, Kärväsniemi	67° 33.620' N, 26° 43.992' E	188.0	6.3	x	x
HI-1, Hietakangas	67° 32.197' N, 26° 39.762' E	183.0	1.0	x	
KU-1, Kuusivaara	67° 30.460' N, 26° 39.429' E	190.0	2.7		
KU-2, Kuusivaara	67° 30.437' N, 26° 40.231' E	203.5	2.1		
KU-3, Kuusivaara	67° 30.662' N, 26° 45.196' E	201.0	3.0	x	x
MU-1, Multaharju	67° 27.039' N, 26° 52.897' E	188.0	1.6	x	

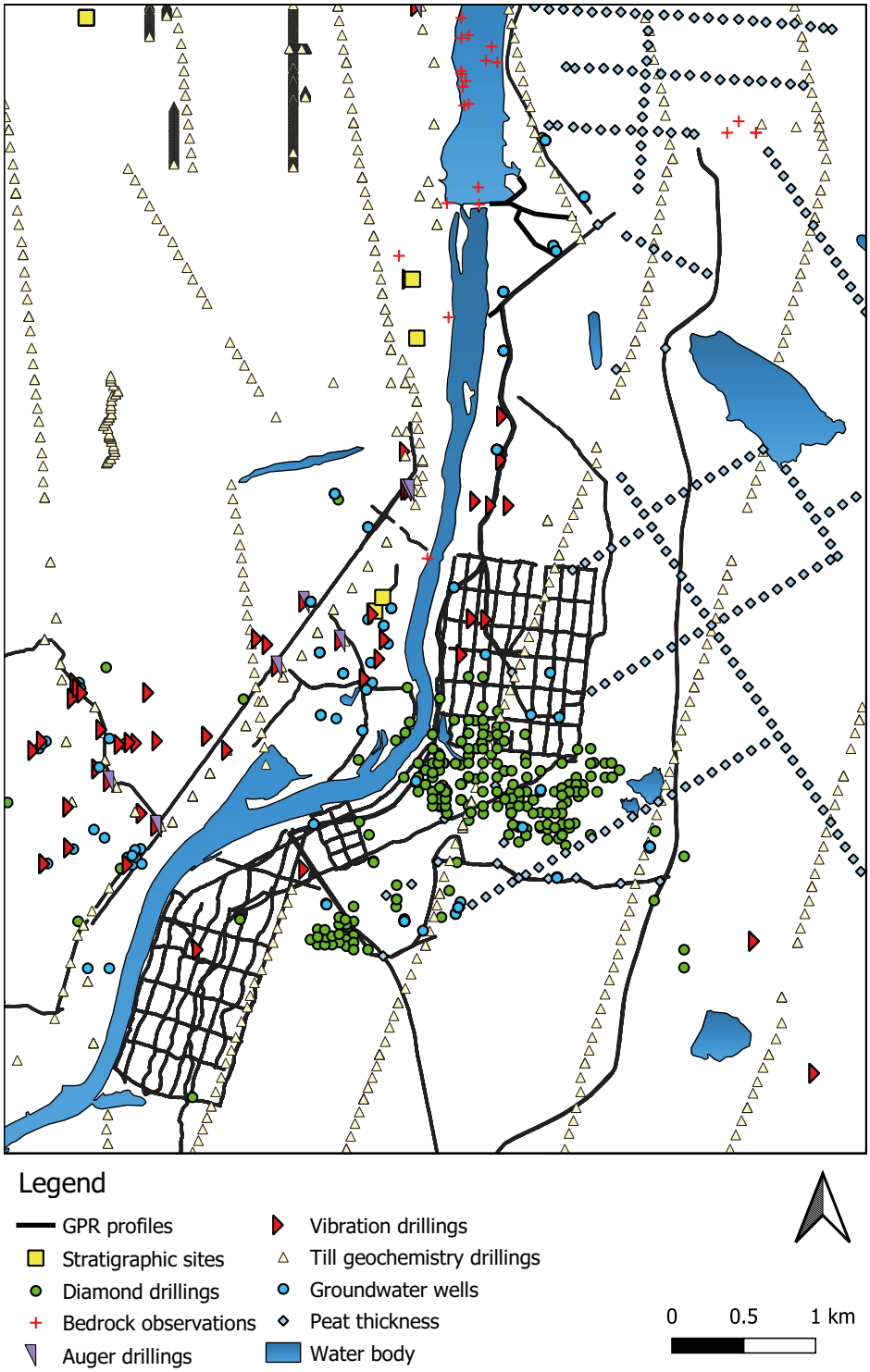

Figure 3. Input data used in GM2020. References for the drillings and stratigraphic sites are listed in Table 1. For location see Fig. 1B. Water body: © National Land Survey of Finland, used with permission.

aries (Fig. 4). Seven distinct GPR patterns were recognised as GPR facies in the profiles studied, and were named A–F (Fig. 4).

The GPR facies A–C were generally smooth in appearance. Facies A and B were usually easy to identify as representing peat and flood plain sediments, respectively, whereas facies C was difficult to differentiate between sandy till or fine-grained sorted deposits. Facies C was mostly encountered in bedrock depressions and could therefore also represent weathered mantle. The patterned facies D–F were interpreted as representing different types of flowing water/current deposits. Facies G was interpreted as till verified using drilling data. However, till facies lacked the characteristic upside-down V-shaped pattern typical for till (see *e.g.* Pitkäranta, 2009) and had a blurred contact to the bedrock. The selected interfaces (1–5) were used to define the contacts of the units in the 3D models (Fig. 4).

3.4. Three-dimensional (3D) modelling (Papers I, III & GM2020)

The 3D models of this study were generated with the 3D modelling software Leapfrog Geo (versions 2–5, Seequent Ltd.). Leapfrog Geo is a modelling software package aimed at fast implicit modelling. The 3D model generation of Leapfrog is based on contact surfaces that define the upper and lower limit of each geological unit. As Leapfrog required a relative chronology, it was based on the stratigraphic investigations conducted on the Kärväsniemi sections (KN-1 and KN-2) (Table 3) and on earlier studies (*e.g.* Hirvas, 1991; Sarala *et al*., 2015).

Four 3D models of Quaternary sediments and upper bedrock structures were constructed. The 3D models were named as GM0 (Paper I), GM1 and GM2 (Paper III), and the final model, GM2020, is presented in this thesis.

GM0 covered an area of 10.5 km², including the western corner of the Viiankiaapa mire and Kärväsniemi (Fig. 1B). Two extended models GM1 and GM2 covering 48 km^2 (Fig. 1B) were generated for the comparison of groundwater flow patterns within the area. A detailed GPR study (December 2019–January 2020) was conducted to achieve a more detailed structure for GM2020. In total, 2600 observations (from the compiled GIS data of Table 1) were used to generate GM0 (Paper I), whereas 10 613 observations from the GIS databases (Fig. 3) were used as input for the extended GMs (GM1, GM2 and GM2020). The modelling method of GM2020 is described below (Fig. 5), whereas the modelling of GM0, GM1 and GM2 is described in further detail in Papers I and III.

In the GM1 and GM2 models, the GPR facies C was interpreted as "lowest till" (sandy till; Fig. 4), whereas in the GM2020 model, this facies was renamed as a "basal unknown sediment" due to the lack of reference drilling.

In situ chemically weathered bedrock saprolith is divided according to the degree of weathering into saprock (<20% alteration of available weatherable minerals) and saprolite (>20% of the weatherable primary minerals are altered) (Anand & Paine, 2002; Hall *et al*., 2015). In GM2020, saprolite was further divided into sandy (grus) and clay-type saprolite weathering that are linked to weathering intensity (*e.g.* Hall *et al*., 2015). The distribution of clay and grus weathering was based on WIP (Weathering Index of Parker, Parker 1970) calculations from Hall *et al*. (2015) and Raatikainen (2019). Previous GMs only included weathered bedrock and bedrock units.

Grus and clay-type saprolite was underlain by a unit named "fractured bedrock", consisting of a variety of altered bedrock from slightly fractured bedrock to saprock. The thickness of fractured bedrock unit is tentative because of sparse and uneven distribution of drill-core observations. The observed (n = 41) average thick-

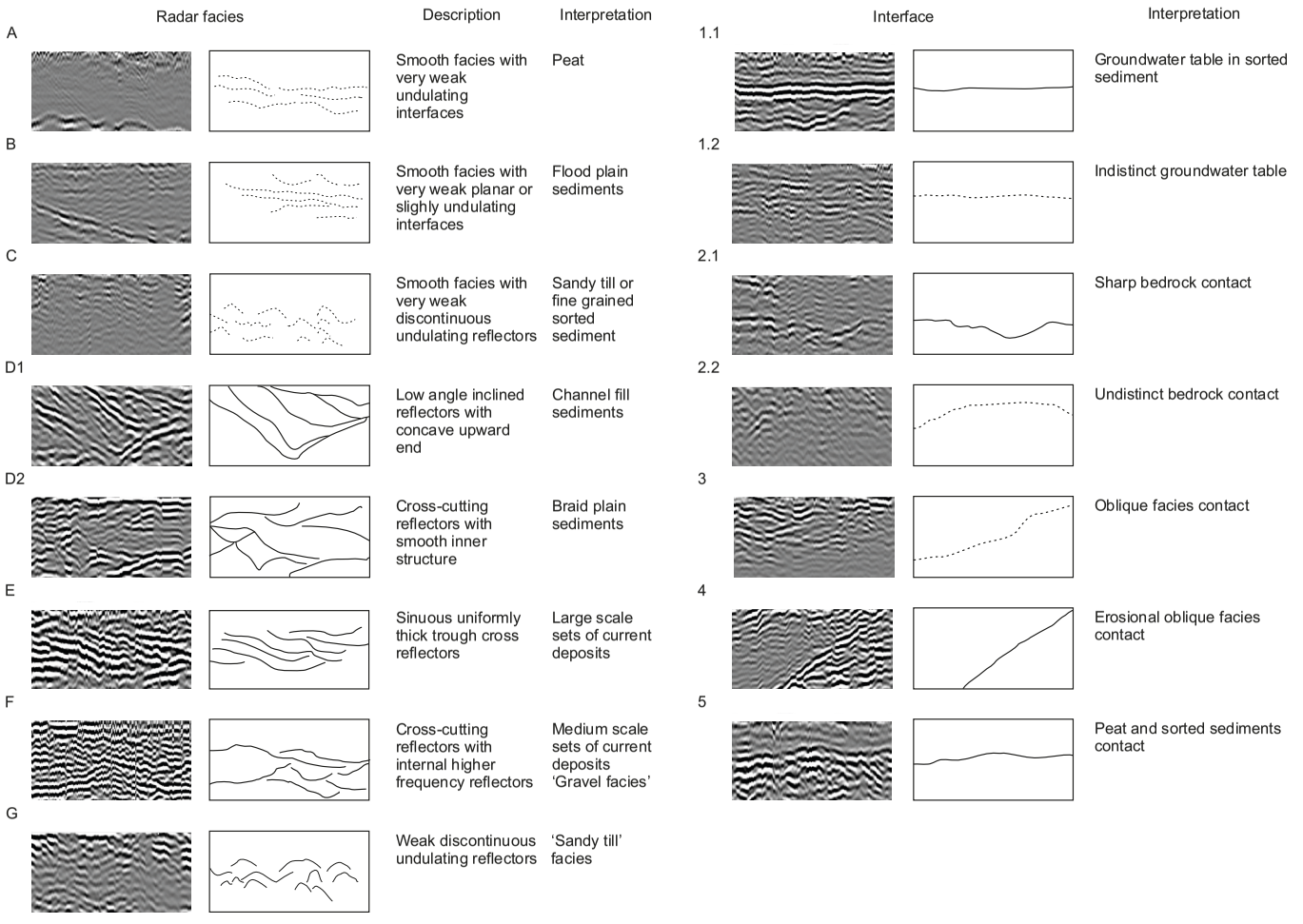

Figure 4. Examples of GPR facies and interfaces of this study with a 100-MHz antenna. The length of each section is 300 metres and the height is 5 metres.

Table 3. Geological units of the geological 3D models (GM), their preliminary correlation with the Kärväsniemi units (KN-2) and NW European and the marine isotope stage (MIS) chronologies.

	KN-2	Chronology	GM0	GM1	GM2	GM2020
River Kitinen		Holocene	x	x	x	x
Peat		Holocene	x	x	x	x
Top deposits	Unit 9	Holocene/Deglacial	x	x	x	x
Upper till	Unit 8	Late Weichselian, MIS 2	x	x	x	x
Middle sorted	Unit 7	Middle Weichselian, MIS 3	x	x	x	x
Middle till	Unit 6	Middle Weichselian, MIS 4	x	x	x	x
Lower sorted	Unit 5 Unit 4	Early Weichselian, MIS 5a	x	x	x	x
Lower till assemblage	Unit 3 Unit 2 Unit 1	Early Weichselian, MIS 5b	x	x	x	x
Lowest sands and gravels		Early Weichselian-Eemian?	x	x	x	x
Lowest till		Saalean?		x	x	
Basal unknown sediment						x
Weathered bedrock			x	x	x[1]	
Clay weathering						x
Grus						x
Fractured bedrock					x	x
Bedrock			x	x	x[2]	x[2]

[1]Divided into clay and grus types with ModelMuse (see Paper III)

[2]As a solid bedrock surface

ness of fractured bedrock was 19 metres (standard deviation (SD) = 20 m; maximum = 83 m). The observations were available only within area the dense diamond drilling area (Fig. 3) covering only 1% of the GM2020 area (48 km²). The thickness data of the diamond drillings were used for the marginal areas of the model where an extrapolated thickness between 10 to 40 metres was used.

The horizontal resolution of the contact surfaces was set to 20 metres, whereas the vertical resolution was not applicable in Leapfrog. The accuracy of the contact surface was set to 0.1, meaning that it had freedom to vary by ±0.1 metres from the control points (polylines, points, drill hole data). The non-continuous sediment units were generated by bending the contact surface in such a way that it formed lens-like 3D units (see Fig. 13 in Paper III).

4. Results

4.1. Results of Paper I

Paper I focuses on visualising the complicated sedimentary architecture and sedimentary environments of the Sodankylä study area.

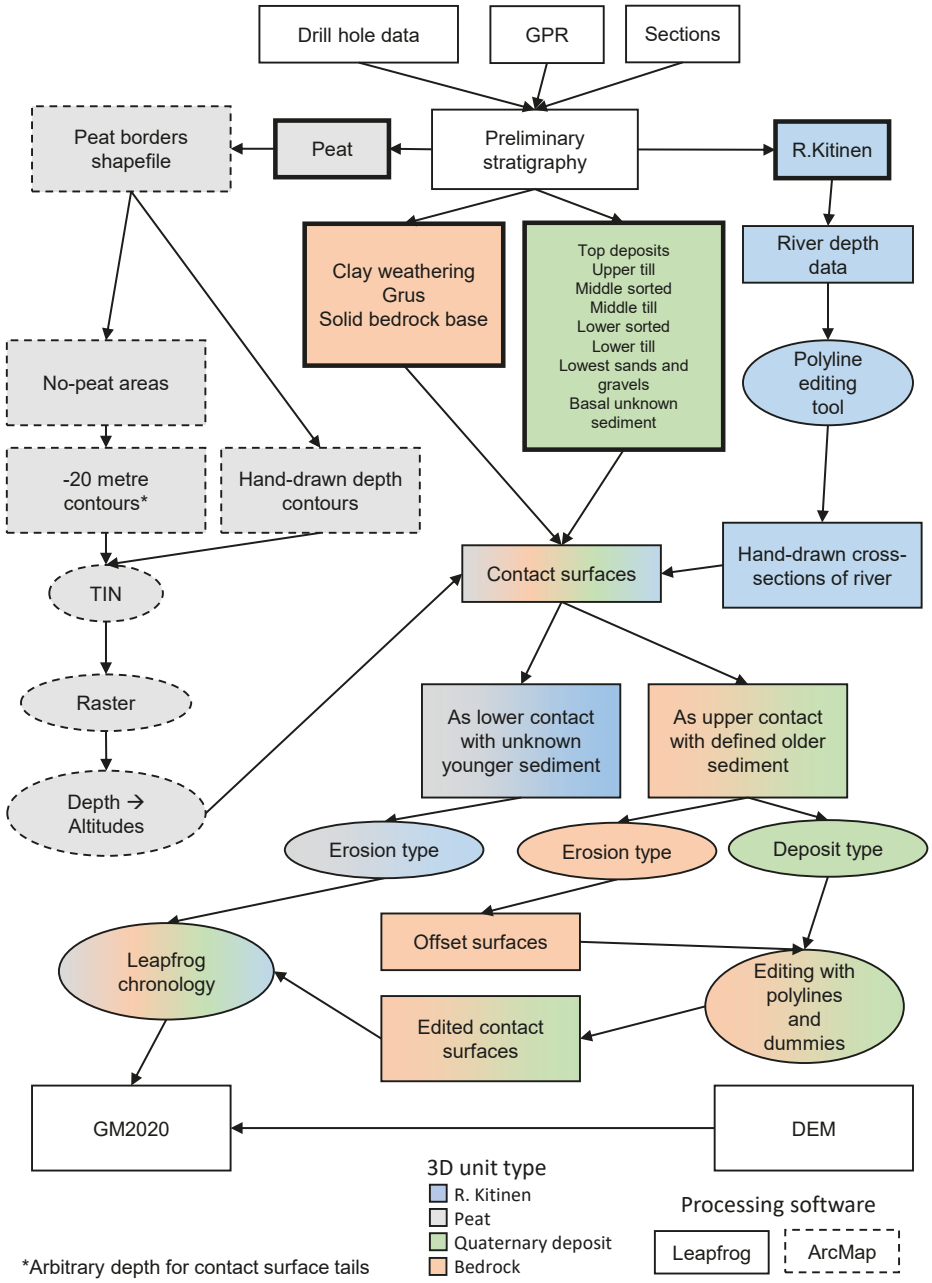

Figure 5. Simplified modelling workflow for the 3D model GM2020 with Leapfrog Geo and ArcMap software. The colour scheme indicates the track of modelling methods of the 3D unit types. The squares depict files that define the 3D units and the ovals depict tools to edit the geometry of the 3D units. Much the same workflow was used in GM0–2 in Papers I and III.

Three till units with four interbedded sorted sediment units were encountered in the area from where GM0 was reconstructed, each having an average thickness of approximately 2 metres. The most complex sediment succession was encountered in Kärväsniemi, whereas

a more simple stratigraphy, typically with only one till bed, was encountered in the elevated areas. The Viiankiaapa mire also revealed a less complex stratigraphy, with organic mire deposits underlain by a sandy unit and till.

Several topographic features and related variations in sediment thickness were observed in the modelled areas. Since the topography of the Sodankylä peneplain is rather smooth, the thickest sediment successions (>15 m) occur in bedrock depressions which were presumably sheltered from glacial erosion. The high bedrock areas seem to locate in the areas where plutonic and volcanic rocks occur, while the low altitude bedrock areas consist of metasedimentary rocks. The depressions in Pahanlaaksonmaa (Fig. 1) and the Viiankiaapa mire are most likely situated in areas of bedrock fracture zones. The thickest sediment succession, containing a maximum of approximately 40 metres of sorted deposits, was encountered in Pahanlaaksonmaa, and in Ropisijankuru (Fig. 1) the sedimentary succession is 35 metres thick and consists of 33 metres of sand beneath the uppermost till unit.

Glaciofluvial and fluvial sands are common in and along the river valleys as seen in the LiDAR-DEM imageries. According to the GM0, the fluvial deposits continue beneath the Viiankiaapa mire. The three sorted sedimentary units of fluvial origin were deposited near the river banks, and were interbedded with till units. This indicates recurrent fluvial activity in the area.

The open dataset of the "Targeting till geochemistry" project was found to be a valuable dataset in the 3D modelling. However, in this dataset, the exact contacts of the units are often unknown, and the bedrock surface model was constructed with the assumption that the depths of the drillings represent the bedrock surface or are close to it. From this, it follows that the bedrock surface model represents the minimum thickness of surficial deposits, and the Leapfrog model (GM0) may therefore underestimate the volume of Quaternary deposits. On the contrary, in areas with sparse geological data, interpolation overestimates the thickness due to the uneven lateral distribution of the input data and high variability in the sediment thickness and bedrock surface altitude within a short distance.

The interlayered till forms perched water tables, and the hydraulic conductivities are highly heterogeneous. The 3D modelling and the Kersilö database indicated that the sorted deposit units of some of the classified aquifers were less uniform, thus making them less profitable as groundwater reservoirs.

4.2. Results of Paper II

Paper II focuses on sedimentological and lithological observations, LiDAR image analyses and OSL age determinations in the River Kitinen valley. The Kärväsniemi sections (KN-1 and KN-2) were divided into nine and Kuusivaara (KU-1–KU-3) into six lithostratigraphical units; Hietakangas (HI-1) and Multaharju (MU-1) were each composed of one unit. Two of the seven sections (KU-1 and KU-2) were excavated down to the bedrock. The lithofacies includes three to four diamicton units interbedded with sorted sediment units and weathered bedrock. The stratigraphy of the Sodankylä area and its correlation to the late Middle and Late Pleistocene NW European and MIS chronostratigraphy is presented in Fig. 6; the individual lithofacies are described in more detail in Paper II.

The sedimentological evidence obtained from the River Kitinen valley indicates that glacial ice advanced across the area on at least three separate occasions, in the Early (MIS 5b), Middle (MIS 4) and Late (MIS 2) Weichselian, whereas ice-free conditions persisted during the intervening Odderade (5a) and MIS 3 interstadials.

The lowermost diamicton unit of Kärväsniemi and Kuusivaara (KN Unit 1; KU Units 1–2)

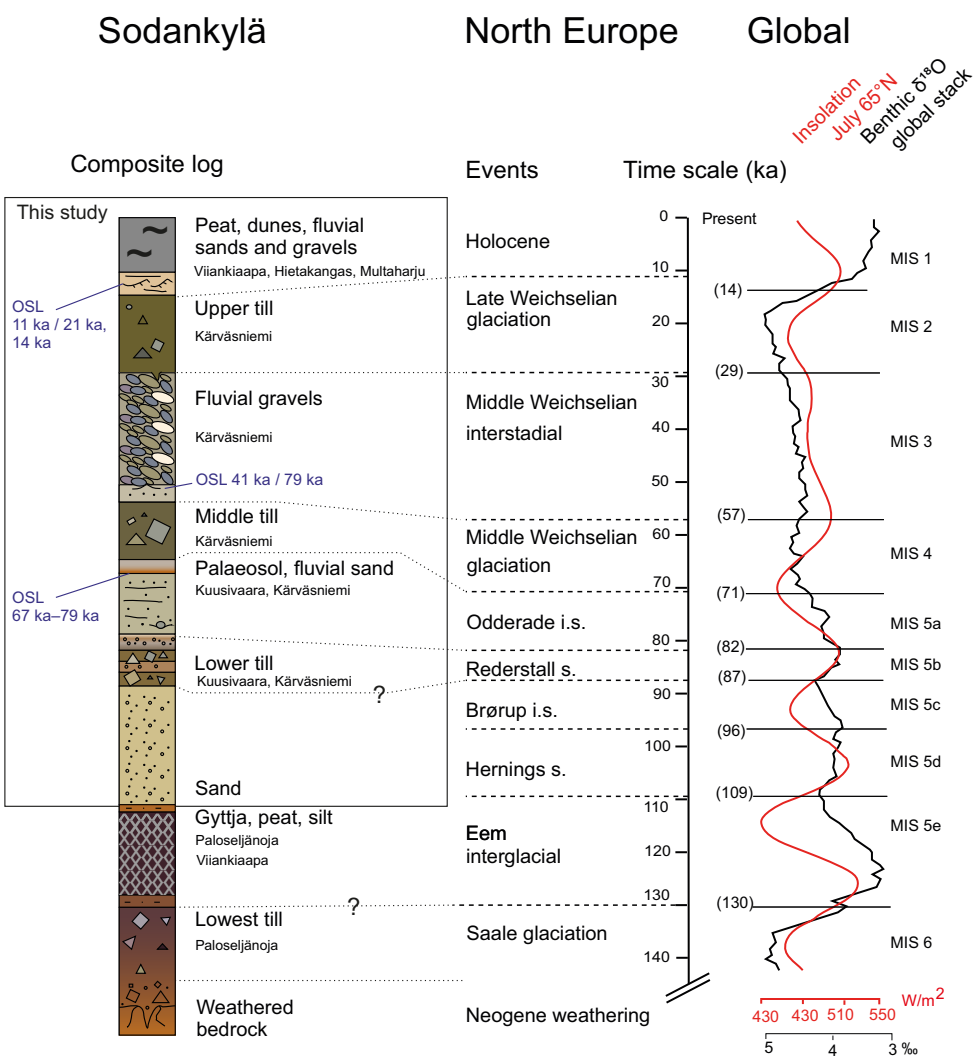

Figure 6. Composite stratigraphy of the Sodankylä area (modified after Salonen, 2019) and comparison with the Northern European stratigraphy and global benthic $\delta^{18}O$ data. The square depicts the stratigraphy observed in this study (Papers I–III). The simplified stratigraphy of Paloseljänoja and its correlation is based on Hirvas (1991). The time scale is modified after Helmens *et al*. (2018). The benthic $\delta^{18}O$ data are from Lisiecki & Raymo (2005) and the insolation curve is from Berger & Loutre (1991).

forms a continuous floor in the river valley and was interpreted as representing till deposited by the Early Weichselian glacial ice. The correlation is based on the strong NW-oriented fabrics, widely accepted to represent the Early Weichselian ice-flow direction (*e.g.* Hirvas, 1991; Johansson & Kujansuu, 2005).

Early Weichselian diamictons are overlain by mainly plane-bedded sands and gravels in Kärväsniemi and Kuusivaara. These deposits had features that indicate a proglacial environment, including ice-wedge casts and drop stones in sandy matrix and remnants of palaeosols. The OSL ages (67–79 ka) indicate deposition during the Early Weichselian interstadial, Odderade.

A 30-cm-thick diamicton unit, interpreted

as Middle Weichselian till, was encountered in Kärväsniemi. The till clast fabric and one striated clast indicate an ice-flow direction from the N or NE (20°–15°), which can be compared with the flow directions of "old northern till" described in Johansson (1995). In Kärväsniemi section gravel-rich unit, interpreted as braided river traction lag/bar deposit was the only Middle Weichselian sediment unit encountered in the present study. OSL-samples dated yield ages of 41±9 and 73±12 ka. The bimodal age result indicates poor bleaching but the younger age obtained was considered more likely age for the unit *i.e.* the gravel-rich unit was deposited most likely during the Middle Weichselian at around 40 ka ago.

The Late Weichselian diamictons (KN Unit 8; KU Unit 4) have a scattered distribution over the river valley area. In general, the Late Weichselian diamicton was interpreted as melt-out till, based on the presence of lenses of sorted sediments, the loose packing, and the absence of basal erosion. The till clast fabric from KN-1 had a preferred orientation of clasts from 295°.

The glacial flow-direction analysis suggested that the topographic features of NW–NNW-oriented streamlined bedforms in the Kittilä and Salla areas represent an older bedform swarm than Late Weichselian, probably Early Weichselian (Fig. 7). This would indicate a northern location of the ice-divide zone during the Early Weichselian and a more westerly location during the Late Weichselian. The Middle Weichselian till with N–S-oriented till fabrics together with till-covered eskers related to the subsequent deglaciation suggest a northerly position of the ice-divide zone during the Middle Weichselian. The Late Weichselian glacier was partly cold-based, and local ice streams existed in areas where the till clast fabric analysis show strong orientation of clasts' *a*-axis. All in all, the flow direction analysis indicated prolonged cold basal conditions of the glacier in the Sodankylä area during the whole Weichselian.

The relatively old OSL age from Multaharju (14±3.2 ka) and old radiocarbon (13–16 ka) dates obtained from organic samples from other sites in northern Finland (*e.g.* Heikkinen *et al.*, 1974; Jungner, 1979; Nydahl *et al.*, 1972) may indicate that northern Finland deglaciated earlier than previously thought (*e.g.* Hughes *et al.*, 2016; Stroeven *et al.*, 2016), already during the warm Bølling–Allerød period. If the OSL and radiocarbon dates are reliable, the area was probably partly ice free due to local scattered glaciers. Another likely explanation is poor bleaching of the Multaharju sample.

4.3. Results of Paper III

Paper III focuses on the comparison of two simpler hydrostratigraphic models (HSMs) derived from GM1 and two more complex hydrostratigraphic models derived from GM1 and GM2, respectively, via groundwater flow modelling.

The aim of this study was to evaluate how the modelling results for groundwater flow and recharge/discharge patterns differ when simple or more elaborate HSMs of the Sakatti study site are applied. A workflow for 3D hydrostratigraphic modelling with Leapfrog Geo and flow modelling with MODFLOW-NWT was developed.

Groundwater modelling results indicate that statistical parameters of the residuals between the observed and simulated water tables were rather similar in all HSM groundwater flow models. However, statistical parameters calculated in groundwater monitoring wells with varying screen depths indicated that a more detailed stratigraphy increased the statistical fit. In addition, defects in the GMs could be detected from groundwater modelling results as areas with a poor fit between the observed and simulated groundwater table. Groundwater flow patterns were verified with particle tracking with stable isotope values ($\delta^{18}O$, δD, *d*-excess). The sim-

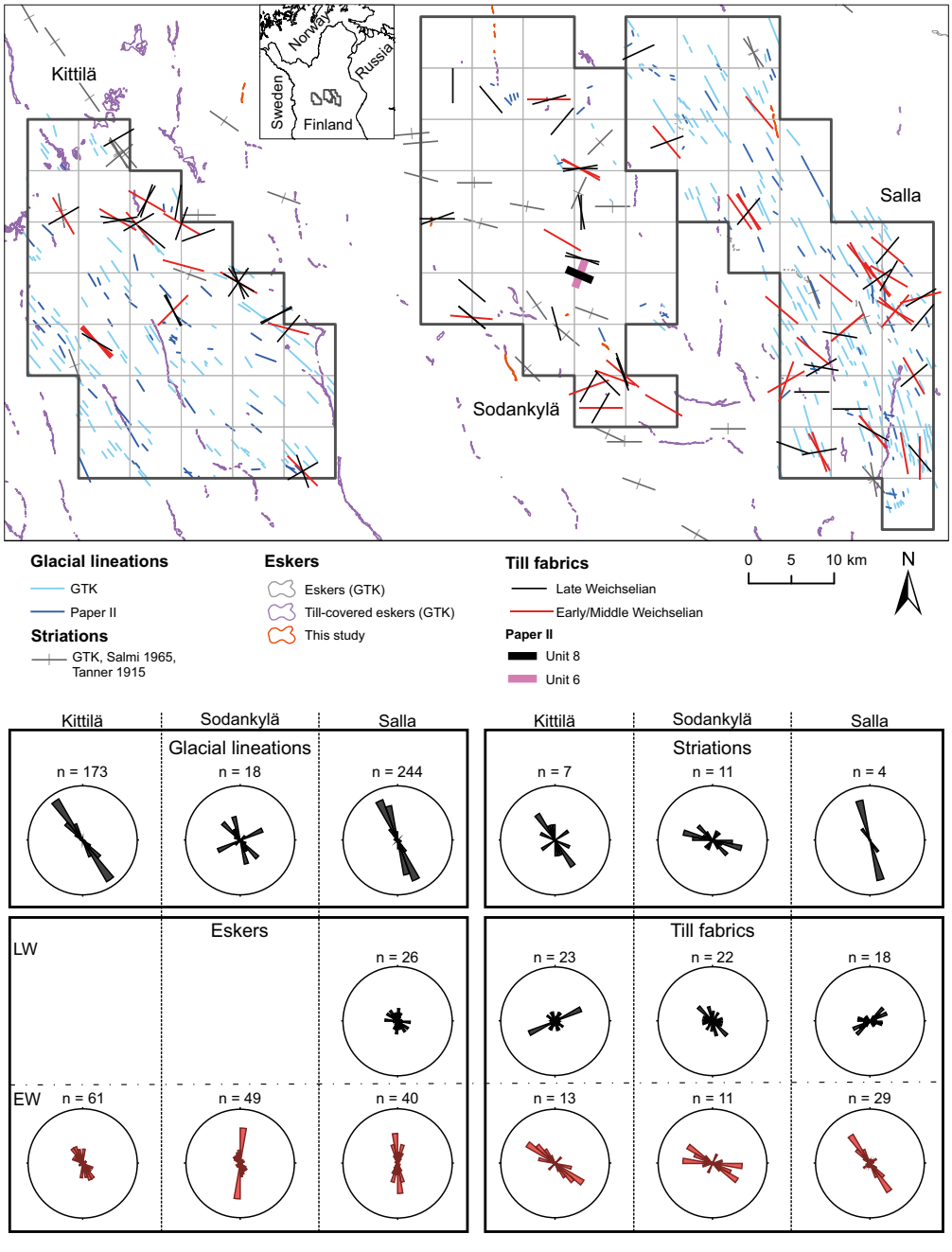

Figure 7. Results of flow direction analysis within the LiDAR inspection areas, Kittilä, Sodankylä and Salla. In eskers and till fabrics of the flow direction analysis, the red colour indicates the Early/Middle Weichselian (EW), whereas black indicates Late Weichselian (LW).

ulated flow paths of the *d*-excess suggested a more complex flow pattern in the complex models compared to the simple models. The simulated flow paths of the complex models were dependent on hydraulic conductivity (*k*-value) variation, and the topography of unweathered

bedrock.

The interbedded zones of low and high conductivity generate more complex recharge and discharge patterns due to an increase in the vertical component of groundwater flow. In the simple models, the groundwater flow lines were mainly subhorizontal, whilst in the complex HSM models, the interbedded low conductivity zones (tills, clay-type weathered bedrock) refracted the groundwater flow lines in a more vertical direction (see Freeze & Witherspoon, 1967) if underlain by a higher conductivity zone (*e.g.* sorted deposits). In the complex models, the groundwater discharge areas reflected the string and flark pattern of the mire more precisely than in the simple models. Moreover, the low conductivity zones acted as a barrier to groundwater flow; the groundwater head rose in the upstream direction and lowered in the downstream direction, regardless of their shape. The aforementioned aspects emphasize that low conductivity zones should be acknowledged in 3D model construction.

Building a complex 3D model should be constructed if enough time and data for the modelling is available. Furthermore, if the study site has high variation in hydraulic conductivities, and a detailed understanding of groundwater recharge and discharge patterns is of research interest, a detailed structure in a 3D model is desirable.

4.4. The geological model GM2020

The final version of the GM2020 model was constructed for the basis of a hydrogeological flow model. According to GM2020 model, the bedrock topography ranges 135–206 m a.s.l. (SD = 6.7 m), the average being 180 m a.s.l. The average thickness of the "fractured bedrock" unit is approximately 25 metres, but the unit thickness variates (>20 m) within short distances. Fractured bedrock is overlain by a prominent amount of weathered bedrock, of which the dominant type is grus (Table 4). Approximately one-eighth of the weathered bedrock comprises clay weathering, which forms scattered clusters along the model area, but is absent from the area dominated by fluvial sediments.

The average thickness of Quaternary deposits is 8 metres (SD = 4.3 m), ranging from 0 to 47.8 metres. The average thickness of tills and sorted deposits is about 2 meters (Table 4), except for the "basal unknown sediment", which has a thickness of over 4 metres. The lowest Quaternary sediment units ("lowest sands and gravels" and "basal unknown sediment") fill bedrock depressions and have a higher mean thickness and standard deviation than the overlying units. The most voluminous sorted deposit unit is the "top deposits", whilst the most widespread till unit is the "lower till" (Table 4), both of which cover almost the entire model area. Both "middle sorted" and "middle till" have a limited coverage, being less than 5% of the Quaternary deposits, the "middle till" being limited to Kärväsniemi only. The "upper till" is scattered along the model area, especially in the outwash plain areas (Fig. 8). Till-covered sorted deposits are distributed in the outwash plain areas and scattered beneath the mire-covered areas.

5. Discussion

5.1. Three-dimensional (3D) geological models

5.1.1. Input data for the 3D geological models

The GM2020 model was constructed using information from drillings, outcrops and the GPR sounding results (Fig. 3), as well as exploiting previously published data. The quality of the input data was variable regarding its representativeness, degree of detail and spatial distribution

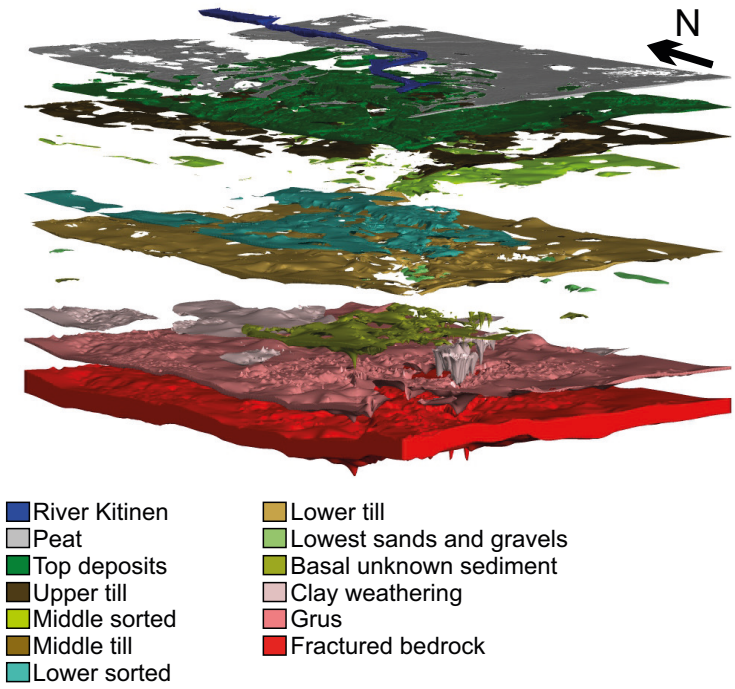

Figure 8. "Exploded view" of the 3D geological model (GM2020) in Sodankylä, central Finnish Lapland. For the location, see Fig. 1B. For the geological units, see Tables 3 and 4. Vertical exaggeration is 10x. The thickness of the fractured bedrock is tentative (also Figs. 11, 12 and 14). See text for further details.

of the data (Paper I).

The information on sedimentary succession from the drillings varied from detailed descriptions of the units and their bounding surfaces (*e.g.* vibration drillings of Leskelä (1971) to the overall thickness of the Quaternary deposits without any information on lithologies (*e.g.* diamond drillings, Fig. 3). The "Targeting till geochemistry" dataset, in turn, included lithological information, but the boundary information was mostly lacking. However, even if there were deficiencies in the lithological data, they were sufficient for modelling purposes and counterbalanced by the dense sampling network.

The input data (drilling, outcrops and GPR) were unevenly distributed within the GM2020 area (Fig. 3). All the outcrops were located west of the River Kitinen. The densest drilling and GPR network was in eastern side of the River Kitinen (Fig. 3), being more scattered in the nature conservation area of the Viiankiaapa mire. This led to a more detailed understanding of the deposits in the river belt compared to the mire areas. In the areas covered by a grid of GPR profiles, it was possible to see a continuum of erosional structures and, in some cases, sedimentary units. In the mire areas, in turn, the isolated GPR profiles lacked crosscutting lines, and the shape and continuity of the depositional structures and elements was, therefore, less evident. The overall interpretation was thus based more on the drill hole data.

Most of the GPR acquisition was performed using both 50 and 100-MHz antennae, enabling the detection of sedimentary units down to 0.25 metres thick at best. Therefore, the vertical resolution was not precise enough to detect thin units such as the Middle Weichselian till in Kärväsniemi (KN Unit 6), although it is possible that a single rugged or undulating interface occurring in the GPR profile represents this till unit. The penetration depth decreases as a function of increasing antenna frequency. In some cases, the GPR did not reach the bedrock contact, but in

Table 4. The statistics of the GM2020 units and their correlation with the units in KN-2 and northern European chronology. Note that the volume percentages are calculated separately for the Quaternary deposits and for the bedrock.

	KN-2	Chronology	Mean (m)	SD (m)	Min (m)	Max (m)	Volume (m^3)	Quaternary deposits/ bedrock (%)
River Kitinen		Holocene	4.0	2.4	0.0	10.6	7.3×10^6	
Peat		Holocene	2.0	1.0	0.0	6.8	5.2×10^7	13.5
Top deposits	Unit 9	Holocene/ Deglacial	2.1	1.7	0.0	10.9	7.8×10^7	20.2
Upper till	Unit 8	Late Weichselian, MIS 2	1.7	1.1	0.0	8.8	5.4×10^7	14.1
Middle sorted	Unit 7	Middle Weichselian, MIS 3	1.4	1.4	0.0	9.8	1.6×10^7	4.1
Middle till	Unit 6	Middle Weichselian, MIS 4	0.5	0.3	0.0	1.0	2.2×10^4	0.006
Lower sorted	Units 4–5	Early Weichselian, MIS 5a	2.3	1.8	0.0	13.9	3.3×10^7	8.6
Lower till	Units 1–3	Early Weichselian, MIS 5b	2.9	2.0	0.0	13.5	1.2×10^8	30.9
Lowest sands and gravels		Early Weichselian-Eemian?	2.6	2.1	0.0	10.3	3.9×10^6	1.0
Basal unknown sediment		Saalean?	4.5	4.1	0.0	38.3	2.9×10^7	7.6
Clay weathering			2.5	3.1	0.0	49.5	2.3×10^7	1.5
Grus			6.0	2.6	0.0	41.5	2.6×10^8	17.4
Fractured bedrock			25.6	8.2	0.0	76.5	1.2×10^9	81.0

general, the penetration depth was adequate for the Quaternary deposits in the GM2020 area. When the GPR method is used, two interlinked uncertainties have to be considered. One is the estimation of electromagnetic wave velocities through the subsurface and the other is the interpretation of sedimentary units and elements from GPR sounding data. The sedimentary unit thicknesses extracted from the GPR profiles are susceptible to errors in time-to-depth conversions and the central frequency of the antenna and antenna separation. Especially in groundwater saturated areas, the errors in time-to-depth conversions may result from erroneous interpretations of the sedimentary units (Neal, 2004). Due to the sensitive environmental restrictions, GPR acquisition in this work was carried out by skiing during the winter. The snow depth in the study area was 60–80 cm, which may have hampered the recognition of the topmost sedimentary units.

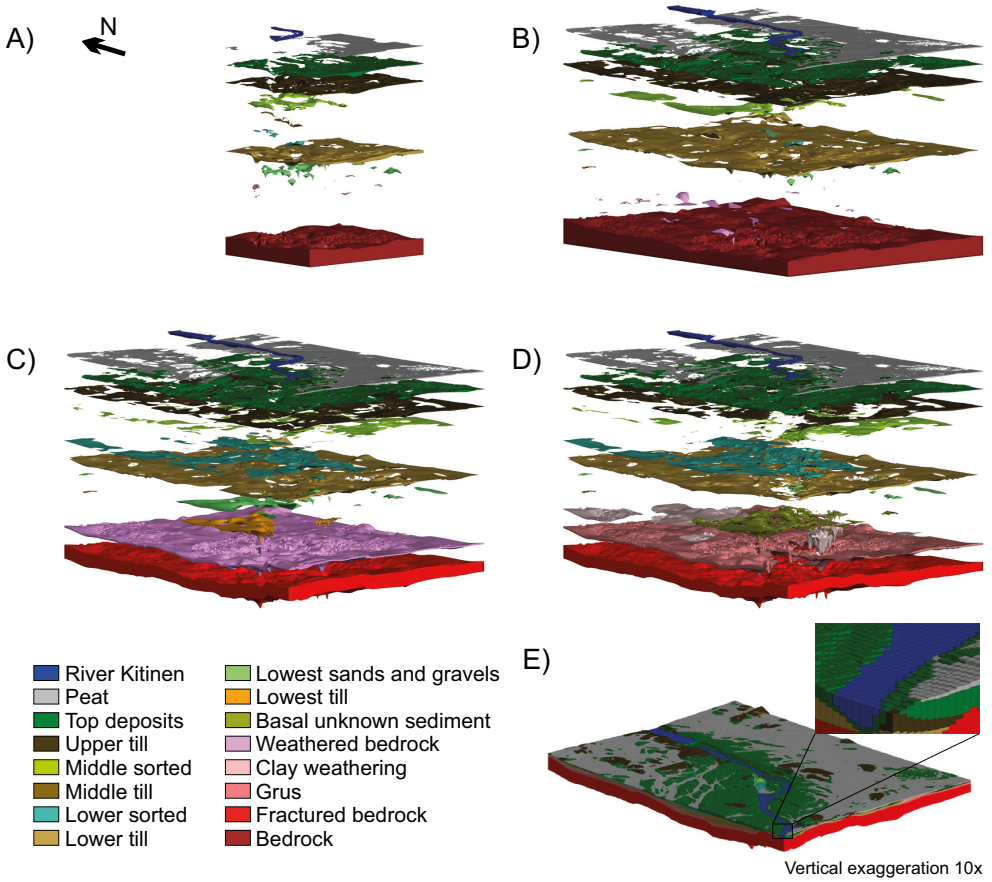

Figure 9. Four versions of the geological model in the Sakatti area. A) GM0 (Paper I). B) The extended model GM1 (Paper III). C) The updated extended model GM2 (paper III). D) The final model (GM2020). E) GM2020 converted into a MODFLOW grid (HSM2020) with the Hydrogeology tool of the Leapfrog software.

5.1.2. Constructing 3D geological models

During this study, four geological models were constructed (GM0, GM1, GM2 and GM2020; Fig. 9). While GM0–GM2 leaned more on the drill hole data, the gridded GPR was utilized in the GM2020 model to gain a better understanding of sedimentary unit architecture and continuity (Fig. 3). The models GM0 and GM1 were similar, but GM1 covered a larger area. In addition to the units modelled in GM1, fractured bedrock was added to GM2. In GM2020, the weathered bedrock was divided into grus and clay weathered zones. The GM2020 model is also more complex than the earlier versions including more units and data (*i.e.* gridded GPR data, see Fig. 3) to increase the model accuracy. The detailed GPR study did not have a drastic effect on the unit volumes. However, the average thickness of the Quaternary deposits in GM2020 is higher and, in places, the bedrock topography is lower compared to that in the earlier GM versions.

According to Hudon-Gagnon *et al.* (2015), the simplification of a model does not markedly alter the model results, which also supports the usage of simpler models. However, more complex GM models are necessary if complex hydrogeological flow routes are anticipated, as in mire

areas or groundwater-dependent ecosystems. For example, in the 3D groundwater flow model of Artimo (2004), the complex routes of mine water leachates required a more complex model to obtain satisfactory results.

The GM2020 model was constructed in order to build a hydrogeological flow model. Therefore, revealing the architecture of individual units with differing hydrological conductivity (*k*-value) is essential; the units should be generated to correspond to the hydrogeological properties. Paper III demonstrates that especially in hydrologically sensitive areas, such as in river banks with a high hydraulic gradient, increasing the complexity and accuracy of the GM has a large local effect on the groundwater flow modelling results. Groundwater flow was predominantly horizontal in models in which the Quaternary sediments and bedrock were simplified as one layer per unit. Increasing the hydrostratigraphic detail appeared to improve the fit between the observed and simulated water table and created more plausible groundwater flow patterns.

During the compilation of the input data and construction of the GMs, it became evident that lithological observations, including the sedimentary unit boundaries, should be carefully recorded in the drill logs. Reference drillings or outcrops along the GPR profiles would have enabled correlations to be examined between GPR facies and lithological units and would, therefore, have enhanced the model accuracy. Reliability classification regarding all input data could improve modelling and input data handling (see also Allen *et al*., 2008). While Leapfrog software is suitable for generating the 3D units for a groundwater flow modelling input grid, geostatistical tools could be used to calculate the heterogeneity, *i.e.* grain-size variation or *k*-values within the 3D units (*e.g*. Sun *et al*., 2019).

5.2. Geological units, stratigraphy and glacial history of the study area

The lithostratigraphical units identified in drill holes, sections and GPR soundings form the basis of stratigraphy and reconstruction of glacial as well as palaeoenvironmental history for the study area. It is well known that Central Finnish Lapland is characterized by evidence of weak glacial erosion with remnants of thick altered bedrock and multiple till units with interlayered sorted deposits (*e.g*., Hirvas *et al*., 1977; Pulkkinen, 1983; Hirvas, 1991; Kleman *et al*., 1997). Central Finnish Lapland has been covered by multiple glaciations during the Pleistocene and was part of Eurasian ice sheet complex (Svendsen *et al*., 2004; Batchelor *et al*., 2019). In this region, up to six tills units are found (Hirvas *et al*., 1977; Hirvas, 1991; Helmens *et al*., 2000; Johansson *et al*., 2011; Helmens, 2014; Salonen *et al*., 2014b; Lunkka *et al*., 2015; Howett *et al*., 2015; Sarala *et al*., 2015), interpreted as having been deposited during the Saalian and the Weichselian glaciations. However, in most cases, two tills beds (till bed II and III by Hirvas (1991)) have been encountered, which have conventionally been correlated to the Early and Late Weichselian. This study revealed up to 48 metres of Quaternary deposits, including three till units with interbedded sorted deposits of fluvial origin in the Sodankylä area (Paper II).

5.2.1. Weathered and fractured bedrock

Central Finnish Lapland and northern Sweden are areas of exceptional glacial preservation (Hirvas, 1991; Ebert *et al*., 2015). In these areas, including the present study area, the bedrock contact to the overlying Quaternary deposits is not sharp but shows a zone of fractured and gradually altered weathered bedrock (Virkkala, 1955; Hirvas *et al*., 1977; Hyyppä, 1977, 1983; Hirvas, 1991; Hätterstrand & Stroeven, 2002; Hall *et al*., 2015). The GM2020 model distinguish-

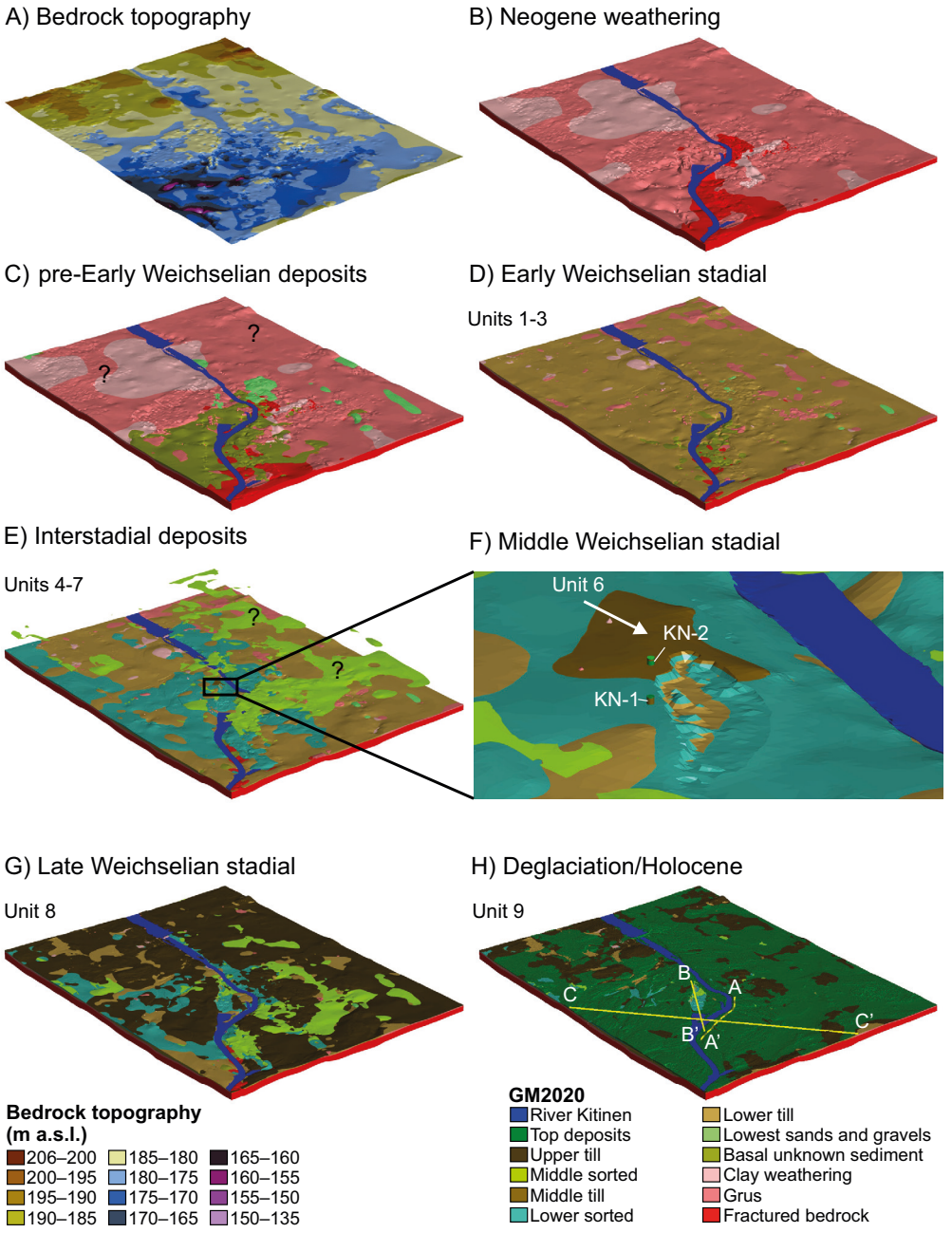

Figure 10. Distribution of the 3D modelled units in GM2020. Corresponding units in D–H are from Section KN-2 at Kärväsniemi. Unit 7 (Middle sorted of the GM model) is in an "exploded position" in E. F) A closer view of limited distribution middle till (unit 6). The question marks indicate areas of uncertain distribution.

es “fractured bedrock”, grus and clay types of weathered bedrock as individual units in the uppermost bedrock zone (Fig. 10). The model suggests that fractured bedrock is the thickest (>50 m) at the bend of the River Kitinen and the thinnest to the west of Viiankiaapa (Figs. 10 and

11). However, due to restricted information on the fractured bedrock unit, the thickness may be overestimated. It is likely that the thickness of the fractured zone shows more spatial variability than presented in the GM2020 as a result of different lithologies and high angle dip of schistosity in bedrock, especially in areas where fractures (joints and faults) are abundant.

Upwards in the altered bedrock zone, the fractured zone gradually changes into weathering grus. Grus-type weathering dominates in the Kitinen river valley area, being on average 6 metres thick (Table 4). Similarly to the fractured zone thicknesses in GM2020, the average thickness of grus may be overestimated and may form a more uneven surface than presented in the model. Grus is overlain by a chemically altered clay-type unit that exists in scattered areas within the study area (Fig. 10B) (Hyyppä, 1977; Rask & Lintinen, 2001; Hall *et al*., 2015). According to GM2020, the average thickness of the clay-type unit is 2.5 metres but is up to 50 metres thick in the brecciated zones. The thickness of both the grus and clay weathering type has a degree of uncertainty due to the lack of reference data and variations in local lithologies.

Fractured bedrock is exposed in places in the river channels, suggesting the removal of weathered material by fluvial activity (Fig. 10B). The scattered distribution of clay weathering in the area may result from a limited time to develop (Hall *et al*., 2015). Alternatively, the clay weathering may have been partly eroded by glacial erosion and mixed in glacial drift (*e.g*. Hirvas *et al*., 1977; Peuraniemi *et al*., 1997). This is further supported by the similarity of chemical compounds in the clay fraction of till and weathered bedrock (Hirvas *et al*., 1977).

5.2.2. Early Weichselian glaciation (KN Units 1–3, KU Units 1–2)

The Early Weichselian sub-stage has been correlated with marine isotope stages (MIS) 5d–5a (Lisiecki & Raymo, 2005; Helmens, 2014), and Greenland chronology GI-25–GS-20 covering a time interval of *ca*. 115–71/74 ka (Martinson *et al*., 1987; Dansgaard *et al*., 1993; Giaccio *et al*., 2012; Rasmussen *et al*., 2014; Obrochta *et al*., 2016). The climate during the Early Weichselian fluctuated from stadial to interstadial conditions (*e.g*. Johnsen *et al*., 1992; Dansgaard *et al*., 1993; North Greenland Ice Core Project members, 2004), affecting the global sea level and extent of the SIS (Shackleton, 1987; Cutler *et al*., 2003). The Early Weichselian was divided into two stadials (MIS 5b and MIS 5d) and two interstadials (MIS 5a and MIS 5c) (Shackleton, 1969; Woillard, 1978; Behre & Lade, 1986; Dansgaard *et al*., 1993). During the latter stadial (MIS 5b), known as the Redenstall stadial, the glacial extent was more widespread (Helmens *et al*., 2000, 2009) than during the previous stadial (MIS 5d), Herning stadial. Various studies have suggested that at maximum, the SIS extended from Scandinavian mountains to the northern parts of Russian Karelia (*e.g*. Siegert *et al*., 2001; Svendsen *et al*., 2004). In Finland, during the Redenstall stadial (MIS 5b), ice sheet is interpreted to have covered northern Finland, leaving southern Finland ice-free (*e.g*. Nenonen, 1995; Svendsen *et al*., 2004).

The lowest till units (KN Units 1–3, KU Units 1–2; "lower till" in GM2020) in the present study area are correlated with the Early Weichselian Redenstall Stadial (MIS 5b) based on four OSL ages obtained from the overlying sorted sediment units (KN Units 4–5 and KU Unit 3). This study suggests that Early Weichselian till is widely distributed, being the most voluminous unit within the GM2020 area, and is on average three metres thick (Fig. 10D; Table 4). While Units 1–3 were the lowermost units observed in the outcrops (Paper II), the GPR profiles and drillings indicated that underlying de-

posits exist within the GM2020 area, especially in the bedrock depressions. These units below the Early Weichselian tills, the "basal unknown sediments" of GM2020, typically consisted of sorted sediments, but fine-grained to sandy tills were also observed, which may have been deposited during Saalian glaciation (*cf*. Hirvas, 1991). On the other hand, the GPR facies of the "basal unknown unit" resembles that of weathered bedrock in Kuusivaara. Therefore, the nature of the "basal unknown unit" occupying the deepest depressions remains unresolved.

In Paper II, KN Units 1–3 ("lower till") were correlated with the Early Weichselian till bed III of Hirvas (1991), which in general has till clast fabrics indicating ice flow direction from between WNW to NW (Fig. 7). There is a consensus that the Early Weichselian ice-flow direction was mainly from the NW (Hirvas *et al*., 1977; Hirvas, 1991; Johansson & Kujansuu, 2005), also supported by the flow direction analysis presented in Paper II. The streamlined feature pattern visible in the DEM (see Fig. 7) coincides with the orientation of the Early Weichselian till clast fabric, supporting the strong depositional and erosional effect of the Early Weichselian stadial (Paper II). Till clast fabrics in central Finnish Lapland suggests that the ice-divide zone during the Early Weichselian was located northwest of the study area. The NW–SE directional esker chains that are common in the Kittilä and Salla areas are inherited from the Early Weichselian deglaciation (Johansson & Kujansuu, 2005). These eskers are often till covered and considered as erosional remnants of continuous eskers (Johansson & Kujansuu, 2005) (Fig. 7). Some of the esker chains are more than 100 km in length and are prominent in size (up to 25 metres high). Such long meltwater systems could indicate very steady input regimes (see Greenwood *et al*., 2017) during the Early Weichselian deglaciation.

While the correlation is based on the similarity (grain size distribution and colour) of the till units and similar till clast fabric, actual age control is lacking. Age control of Early Weichselian till is often derived from overlying sorted sediment units with ages ranging 108–60 ka (Paper II; Helmens *et al*., 2007b; Helmens, 2014; Lunkka *et al*., 2015; Sarala *et al*., 2015), but age control of the underlying sorted deposits in northern Finland is poor (Helmens *et al*., 2007a, 2018). Moreover, relatively old OSL ages (<200 ka) have been obtained from till-covered sorted deposits (Auri *et al*., 2008; Putkinen *et al*., 2020), which suggests that Saalian tills have also been preserved at some sites. Pre-Weichselian, possibly Saalian, tills exist in central Finnish Lapland, *e.g*. Sodankylä (Hirvas, 1991) and in western Finnish Lapland, at Kittilä (Aalto *et al*., 1992) and Kolari (Rautuvaara, Lunkka *et al*., 2015).

5.2.3. Middle Weichselian glaciation (KN Unit 6)

The Middle Weichselian is defined to cover a time interval of *ca*. 71/74–28 ka and is correlated with MIS 4–MIS 3 (Lisiecki & Raymo, 2005; Svensson *et al*., 2005; Obrochta *et al*., 2016) and Greenland chronology GS-20–GI-3 (Giaccio *et al*., 2012; Rasmussen *et al*., 2014; Obrochta *et al*., 2016). Previously, it was thought that northern Europe was covered by the SIS throughout the Middle Weichselian (*e.g*. Hirvas, 1991; Sutinen, 1992). However, terrestrial evidence such as a radiocarbon ages obtained for a deer antler (*Rangifer tarandus*) from Tornio (Siivonen, 1975) and a mammoth molar (*Mammuthus primigeniuis*) from Iijoki (Ukkonen *et al*., 1999), together with other finite radiocarbon dates of *ca*. 40 ka from subtill organic material in central Finnish Lapland (Hirvas, 1991), suggest restricted ice sheet distribution during the second half of the Middle Weichselian (MIS 3) (Ukkonen *et al*., 1999, 2007). The existence of

ice-free conditions in Central Finnish Lapland is further supported by the OSL ages ranging 60–25 ka from subtill sorted deposits from Sokli and Sodankylä (Paper II; Helmens *et al*., 2007a, b, 2018). The sediment record in western Finnish Lapland indicates two separate glacial advance during the Middle Weichselian, followed by ice-free conditions (Howett *et al*., 2015; Lunkka *et al*., 2015). The reconstructions of the extent of the SIS during Middle Weichselian, are variable. Some reconstructions suggest a continuous ice sheet from northern parts of Middle Europe to the Kara Sea (Svendsen *et al*., 2004), while others depict a more restricted distribution in the EW sector, leaving southern Finland free of ice (*e.g*. Kleman *et al*., 1997; Siegert *et al*., 2001; Räsänen *et al*., 2015).

While a terrestrial record of the Middle Weichselian stadials has been observed in western Finnish Lapland (Howett *et al*., 2015; Lunkka *et al*., 2015) and Ostrobothnia (*e.g*. Salonen *et al*., 2008) and in eastern Finnish Lapland (Helmens *et al*., 2007a, b), evidence of Middle Weichselian stadials in central Finnish Lapland is rare. However, based on the stratigraphical position and the OSL-dates obtained above and beneath the compact till unit (Unit 6, "middle till") in the Kärväsniemi section, it was concluded that the "middle till" was deposited during the Middle Weichselian stadial between *ca*. 67–40 ka (Paper II). In central and eastern Finnish Lapland, evidence of only one Middle Weichselian glaciation (MIS 4) occurs in the sediment record (Paper II; Helmens *et al*., 2007a, b, 2018) whereas deposits related to the two Middle Weichselian stadials (MIS 4 and MIS 3) have been observed in western Northern Finland (Howett *et al*., 2015; Lunkka *et al*., 2015). This implies that the central and eastern parts were covered by one glaciation (MIS 4), whereas two glacial advances occurred in western parts of northern Finland during the Middle Weichselian.

Unit 6 of section KN-2 in Kärväsniemi was interpreted as representing lodgement till deposited during the Middle Weichselian glaciation (MIS 4). This till unit is correlated with diamicton unit in the Sokli sequence (Helmens, 2014; Helmens *et al*., 2018) and diamicton units in Hannukainen and Rautuvaara (Howett *et al*., 2015; Lunkka *et al*., 2015). According to two till clast fabric measurements and one observation of a striated boulder, the Unit 6 in KN-2 was deposited by a glacier flowing from N/NNE. Similar ice flow direction data were also obtained from Savukoski (Johansson, 1995), from the "Suas till" (Sutinen, 1992, and references therein) in Kittilä, NW Lapland, and from the till overlaying the Maaselkä interstadial sediments (Hirvas, 1991; Rossi, 1991). The results of this study together with the results of Sutinen (1992), Johansson (1995) and Salonen *et al*. (2014b), suggest that the main ice flow during the first glacial advance of the Middle Weichselian (MIS 4) was initiated in northern Scandinavian mountains. Furthermore, this would indicate that the ice-divide zone during the Middle Weichselian was situated north of the study area. From this it follows that there must have been another ice dome area north of the present study area.

A glacier flow from north is further suggested by the till-covered esker chains (see Fig. 7) that are often small (<10 m) and consist of esker core material (Johansson & Kujansuu, 2005). The N–S oriented esker chains indicate a meltwater system related to the Middle Weichselian deglaciation (Sutinen, 1992; Johansson, 1995). One of these eskers has an OSL age of 65±13 ka (Johansson & Kujansuu, 2005) corresponding the Middle Weichselian stage. The esker chain pattern indicates the presence of two ice lobes in Central Finnish Lapland: one north-westerly (see Sutinen, 1992) and another north-easterly (see Johansson, 1995). The till fabric of Unit 6 of KN-2 would thus indicate a glacier flow of

the north-eastern lobe.

Although the lateral continuity of the Middle Weichselian till in the GM2020 model was restricted, the unit may, in fact, be laterally more continuous. The limited thickness (30 cm in the Kärväsniemi sections) may have prevented its detection in the GPR profiles. However, based on the absence of Middle Weichselian till in adjacent sections (Fig. 10F), as well as in the GPR profiles, it seems likely that the unit is either thin and scattered or nonexistent elsewhere in the study area.

5.2.4. Late Weichselian (KN Unit 8, KU Unit 4)

The Late Weichselian is defined to cover the time interval between *ca*. 28 ka and 11.7 ka (Lisiecki & Raymo, 2005; Rasmussen *et al*., 2006, 2014), comprising the LGM *ca*. 22 ka (Patton *et al*., 2016) and subsequent deglaciation. The Late Weichselian stage is correlated with MIS 2 (*e.g*. Emiliani, 1961; Martinson *et al*., 1987; Dansgaard *et al*., 1993; Lisiecki & Raymo, 2005) and Greenland isotope stage GS-3 (Andersen *et al*., 2005; Rasmussen *et al*., 2008). During the Late Weichselian, the SIS attained its largest extent in Eurasia during the Weichselian stage and covered Fennoscandia and northern parts of central Europe (Kleman *et al*., 1997; Svendsen *et al*., 2004; Hughes *et al*., 2016), having the most extensive distribution of Weichselian glaciations.

In the study area, the Late Weichselian till (Unit 8 in KN-1 and KN-2 and Unit 4 in KU-1–3), and the "upper till" of GM2020, forms a scattered, rather thin (<3 m) and loose unit in the GM2020 model (Fig. 10G). The till was present in the outcrops on the western side of the River Kitinen, but was less evident in the GPR profiles on the eastern side of the river, indicating that the unit is sporadically occurring or absent. Due to the thinner average thickness of the unit, it may have been that the Late Weichselian glaciation had a weaker erosional potential than Early Weichselian glaciation (Paper II). Low sedimentation rates and minor glacial erosion are also suggested by the 3D thermomechanical model (Patton *et al*., 2016, 2017) that yields low ice surface velocities for the central Finnish Lapland during the Late Weichselian. The Late Weichselian till unit is interpreted as representing melt-out till, and occasionally both supraglacial melt-out and subglacial lodgement till occurs. According to GM2020, the till unit may continue beneath the mire areas and form a blanket over the higher ground. However, GPR studies and field investigations indicate that the "upper till" is occurring sporadically or missing in the areas of former braid plains as a result of glaciofluvial/fluvial erosion during/after the last deglaciation (Figs. 10G, 11 and 12). Based on its stratigraphical position, the "upper till" is correlated with the Late Weichselian till beds I and II of Hirvas (1991) (Paper II).

The study area is located directly south of the Late Weichselian Kolari–Kittilä–Saariselkä ice-divide zone (*cf*. Johansson *et al*., 2011; Sarala, 2005; Putkinen *et al*., 2017; ice divide in Fig. 1), separating the Salla and Kittilä ice-stream lobes to the south from the Inari and Enontekiö ice-stream lobes to the north. This ice-divide zone is characterised by deep weathering and weak glacial erosion (Penttilä, 1963; Hirvas, 1991; Ebert *et al*., 2015; Hall, *et al*., 2015). In the Sodankylä area the streamlined glaciogenic features are scarce and show diverging directions (Fig. 7) whereas in the neighbouring Salla and Kittilä areas a northwest orientation dominates. Contrary to the streamlined features, the NW orientation is not visible in Late Weichselian till clast fabrics but indicates ice flow from the W/SW instead (Fig. 7). This further suggests a westerly ice-divide zone (Paper II), and is also consistent with the flow patterns suggested by Kleman *et al*. (1997) placing the Late Weichselian ice di-

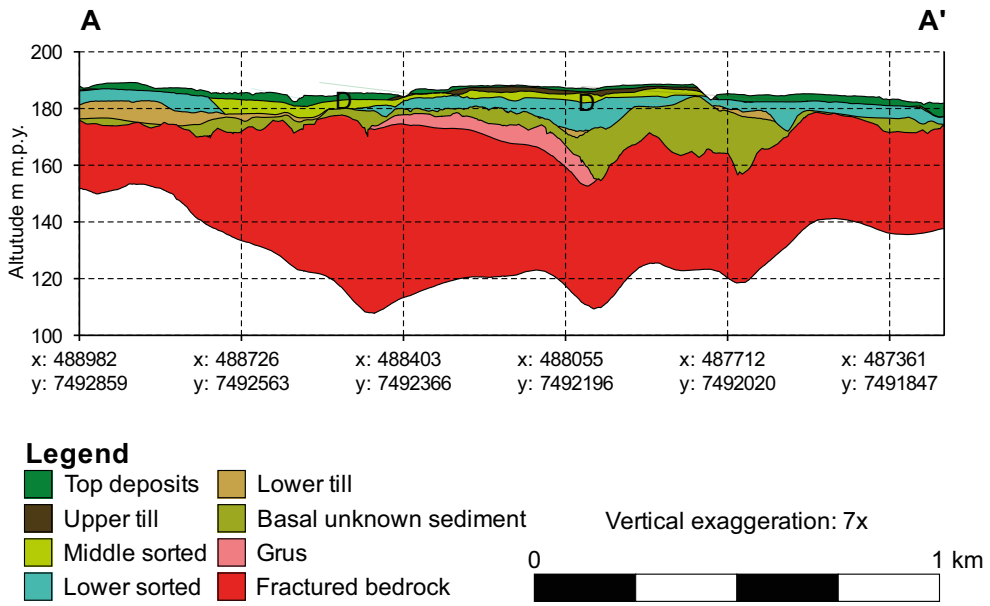

Figure 11. Fence section of GM2020 along GPR profile 112. See location in Fig. 10H. The thickness of the fractured bedrock is tentative. See text for further details.

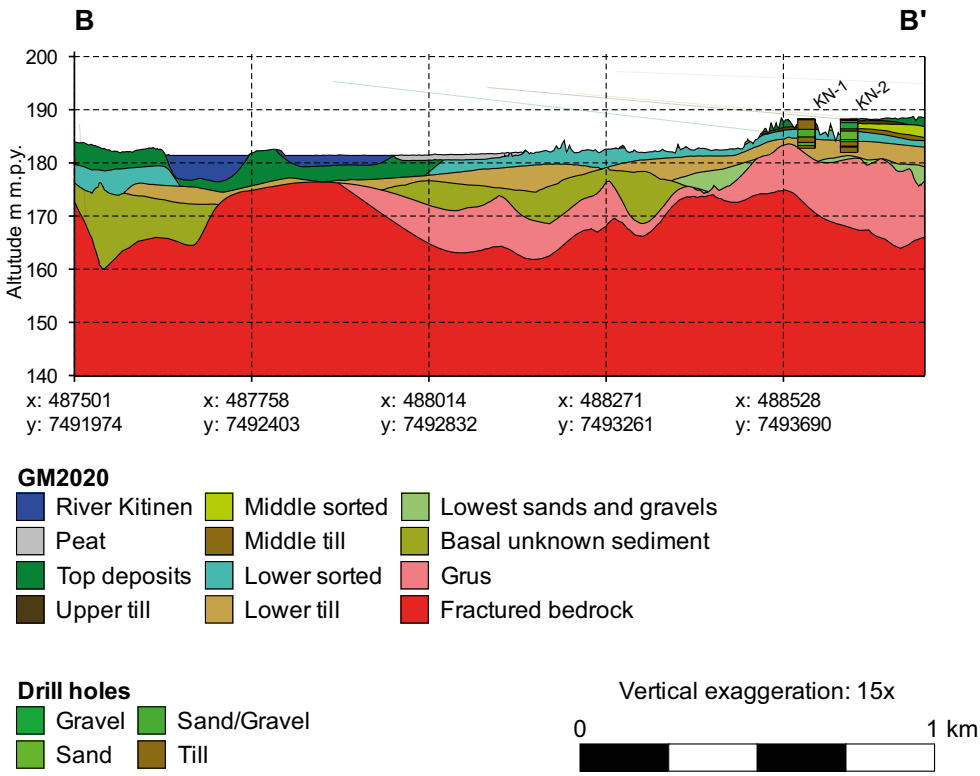

Figure 12. Geological cross-section through KN-1 and KN-2. See location in Fig. 10H. The thickness of the fractured bedrock is tentative. See text for further details.

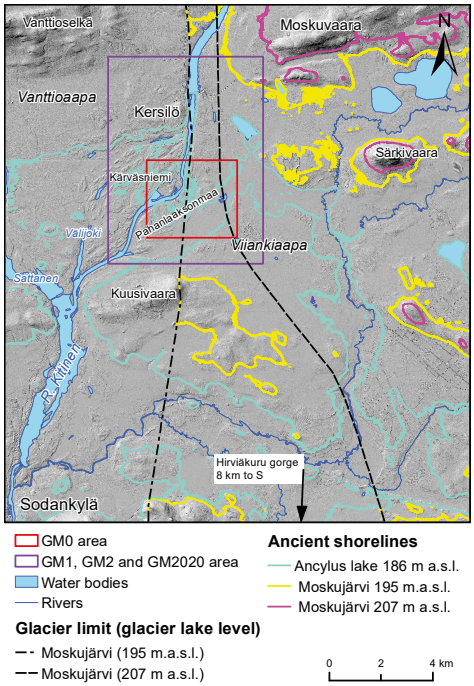

Figure 13. Glacial lakes and estimated glacier limits within the study area. The glacier limits and the glacier lake levels are based on Johansson & Kujansuu (2005). Rivers are modified after Finnish Environment Institute, 2014. Water bodies are modified after National Land Survey of Finland, 2016.

vide in the Gulf of Bothnia. The western location of the last ice divide is further supported by ice flow directions reported from Parkajoki area (Fig. 1), Sweden, at about the same latitudes as the Kolari–Kittilä–Saariselkä zone. In Parkajoki area, the Late Weichselian glacier flow was from the southwest and the Early Weichselian relict landscape indicates a glacier flow from the northwest (see Hätterstränd & Stroeven, 2002). Thus, the Kolari–Kittilä–Saariselkä ice-divide zone may rather be linked to an Early/Middle Weichselian glaciation than to the Late Weichselian glaciation.

While the Late Weichselian SIS ice flow patterns are generally assumed to be seen as lineation features in high-resolution digital elevation models such as the LiDAR DEM (*e.g.* Putkinen *et al.*, 2017), it is not clear whether these subglacial lineation patterns always represent the last ice flow event. Relict landscapes have been observed in Finland that occur as interlobate areas (*e.g.* Punkari *et al.*, 1997). In paper II, it was concluded that the Late Weichselian had a rather weak imprint on the streamlined bedforms, not only in the Sodankylä area but also in the Kittilä and Salla areas. The Late Weichselian till masks slightly streamlined bedforms that likely represent the Early Weichselian ice flow event (Fig. 7).

5.2.5. Deglacial and Holocene deposits (KN Unit 9, HI Unit 1, MU Unit 1, KU Units 5–6)

Shortly after the LGM, *ca.* 22 ka, the climate shifted towards warmer conditions, and the most drastic shift took place during the Bølling–Allerød time (*ca.* 14.6–12.9 ka) (*e.g.* Johnsen *et al.*, 1992; Lisiecki & Raymo, 2005; Rasmussen *et al.*, 2006; Patton *et al.*, 2017), when the SIS rapidly retreated in its southern sector. After the short warm period, the climate shifted again towards colder conditions during the Younger Dryas (12.9–11.7 ka, Rasmussen *et al.* 2006; Patton *et al.*, 2017), and the continuous end moraines circling Fennoscandia were deposited. (*e.g.* Rainio *et al.*, 1995; Lundqvist & Wohlfarth, 2000; Hughes *et al.*, 2016). Finally, after onset of the Holecene, the remnants of the SIS melted in Scandinavia shortly after 10 ka (Lundqvist, 1986; Kleman *et al.*, 1997; Hughes *et al.*, 2016; Stroeven *et al.*, 2016).

According to Stroeven *et al.* (2016), the deglaciation of northern Finnish Lapland occurred *ca.* 11–10 ka, and within the Sodankylä area, the glacier retreated towards the WNW. The western retreat direction of the SIS during deglaciation (Fig. 13) is further supported by palaeowind directions obtained from dunes visible in the LiDAR DEM.

The Sodankylä area was covered by glacial lakes during the last deglaciation. First, the eastern part of Sodankylä was flooded by the Mosku-

järvi Ice Lake *ca*.10.4 ka ago, when the SIS retreated from the SE and the lake level reached a height of 207 m a.s.l. (Johansson & Kujansuu, 2005, Fig. 13). At that time, the Moskujärvi Ice Lake drained towards the Luiro River valley (Fig. 1). Subsequently, around 10.3 ka ago, when the retreating ice reached the Matarakoski delta (location in Fig. 2B), the level of the glacier lake dropped to 195 m a.s.l. due to the opening of a drainage channel in Hirviäkuru gorge (Figs. 2B and 13) (Johansson & Kujansuu, 2005). Later, *ca*. 10.3–10.2 ka ago, the lowland areas of Sodankylä and southern lowlands of the Salla area were covered by the Ancylus lake water, reaching the height of 186 m a.s.l. (Johansson & Kujansuu, 2005).

In the study area, there are abundant deposits comprising fluvial, lacustrine and aeolian sediments which were deposited during the last deglaciation. In GM2020, these are presented as "top deposits" (Fig. 10H), also including Holocene flood plain sediments. Braid plain and fine-grained flood plain sediments are distributed within a *ca*. 4-km-wide zone along the River Kitinen. Coarse-grained braid plain deposits (Fig. 11 location D; Facies D2 in Fig. 4) are a dominant feature in Pahanlaaksonmaa at altitudes of 183–187 m a.s.l., whereas the fine-grained deposits were encountered behind the levee on the eastern side of the River Kitinen. According to GM2020, the thickness of the flood-plain sediments is variable, but reaches 7–10 metres in the west at Pahanlaaksonmaa and in the south at Kärväsniemi.

The outwash plains along the rivers Sattanen, Kitinen and Jeesiöjoki are deposited around the level of the Ancylus Lake, approximately 186 m a.s.l.. According to Johansson & Kujansuu (2005), the outwash is related to the drainage of glacier lakes north of the study area.

During the last deglaciation, the River Kitinen incised the till-covered beds in Sahankangas (Fig. 14 locations E and F) at levels 181–183 m a.s.l. and 184–186 m a.s.l. After deglaciation, the River Kitinen stabilized its channel to its present position, although occasional flooding (Pääkkö, 2004) resulted in fine sediments settling along the shores of the river. Peat formation of the mire areas surrounding the River Kitinen valley started around 10 ka ago (Suonperä, 2016).

Deglacial deposits observed beneath the Viiankiaapa mire are fine sand or silt of fluvial or aeolian origin. The aeolian deposits may originate from the fluvial sediments along the rivers, *e.g*. Kitinen and Sattanen, since the caps of the outwash plains were exposed during the Ancylus Lake phase.

While the final deglaciation is estimated to have occurred at *ca*. 10.3 ka (*e.g*. Stroeven *et al*., 2016) the OSL ages in this study may indicate an earlier retreat of the SIS, even in the Allerød period (Paper II). Considerable evidence exists that central Finnish Lapland was ice free soon after the onset of the Holocene (Hughes *et al*., 2016). Two age determinations from deglacial sediments obtained in this study suggest that the study area was deglaciated at around 11±2ka ago (Hel-TL04301, Table 2 in Paper II), which is supported by the age of the basal peat in nearby Postoaapa, reported as forming 10.35 ka ago (Mäkilä *et al*., 2013). The deglaciation age obtained from the Multaharju aeolian deposits (14±3.2 ka, Hel-TL04302, Table 2 in Paper II) has a wide scatter, which might reflect poor bleaching of the sediment dated. In addition to the OSL date presented in this study, several age determinations indicating pre-Holocene ice-free environments have been reported from northern Finland: 16.4 ka from Lake Sompiojärvi, Sodankylä (Jungner, 1979); two dates of 13.3. ka and 12.4 ka from a sediment core from Pieni Kankaanlampi, Kemijärvi; 12.4 ka (Heikkinen *et al*., 1974) and 12.9 ka (Nydahl *et al*., 1972) from Parvavuoma, Kittilä; and 11.9

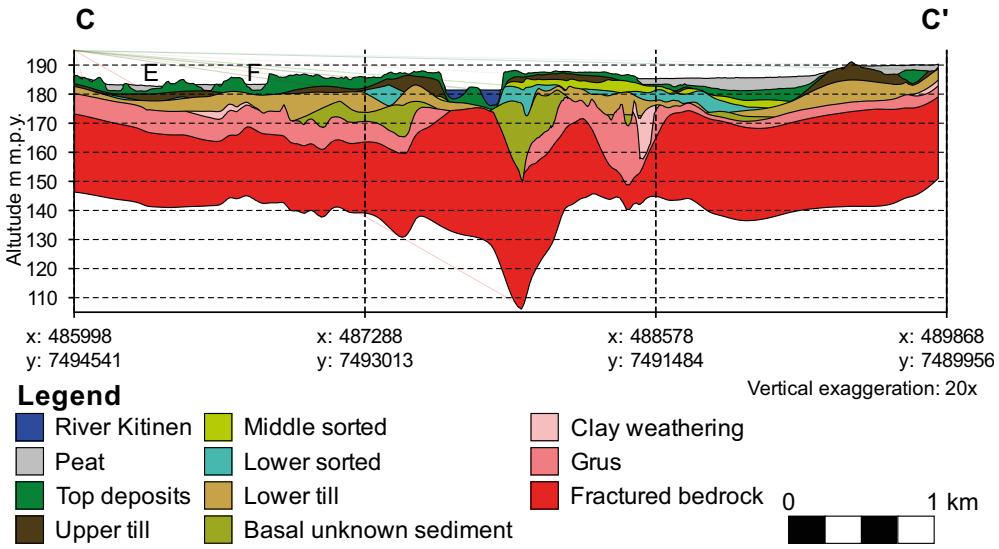

Figure 14. Geological cross-section through Pahanlaaksonmaa and Sahankangas. See location in Fig. 10H. The thickness of the fractured bedrock is tentative. See text for further details.

ka from Lompolojärvi, Pello (Jungner & Sonninen, 1983). Deglaciation of the SIS was rapid during the Bølling–Allerød warm period, which is demonstrated by the rapid retreat of the SIS southern margin (*e.g.* Hughes *et al.*, 2016). The abundance of suggested dates for pre-Holocene ice-free conditions in Finnish Lapland implies that the melting of the SIS might also have been notable in the northern part of the SIS. If the dates are reliable, this suggests that the SIS did not prevail as a uniform ice sheet in the northern part of the SIS during the Bølling–Allerød warm period, but rather as scattered local glaciers with only modest thicknesses.

6. Conclusions

This study presents the 3D geological model (GM2020) from Sodankylä, Northern Finland, that was constructed by combining all existing observations with new drilling data, targeted GPR soundings and LiDAR-DEM imageries.

- According to the GM2020, fractured and *in-situ* weathered bedrock is common in the study area and typically exceeds 20 metres in thickness. The average thickness of Quaternary deposits is 8 metres. The most extensive till unit is the "lower till" representing an early Weichselian glaciation while the Middle Weichselian till unit has a relatively poor lateral and vertical continuity. The uppermost, Late Weichselian till, is patchy and mainly present in topographic highs.
- In areas with complex sedimentation succession as presented in this study, the input data has a major effect on the structure and representativeness of model. The reliability of the model decreases with depth due to the distribution and types of drilling data and attenuation of GPR signal. The GPR soundings were unable to detect thin till units that were, however, detectable in the outcrops.

Based on the observations from the sedimentary successions combined with observations from the drill cores and GPR sounding it is possible to clarify the Weichselian glacial history and sedimentary events that took place in the study area.

- The sediment succession indicates that the SIS overran the study area at least on three separate occasions during the Weichselian Stage; namely during Early Weichselian (MIS 5b), Middle Weichselian (MIS 4), and the Late Weichselian (MIS 2). Interstadial sediments found in the sediment sequence date back to the Early Weichselain Odderade interstadial (MIS 5a) and to one of the Middle Weichselian (MIS 3) ice-free interstadials. The bedrock depression and prolonged cold basal conditions of the SIS have enabled the preservation of thick sedimentary successions (>10 m) of tills and interbedded sorted deposits.
- The Early Weichselian till unit is the most widespread and laterally continuous till unit in the area. The Middle Weichselian till in the study area has a thin and sporadic occurrence. Middle Weichselian (MIS 4) glacier flow from the N/NNE was detected. The OSL age determination suggests ice-free areas in the vicinity of the River Kitinen during the Bølling–Allerod warm period, resulting from a patchy ice cover or rapid deglaciation.

The examination of the Weichselian ice-flow directions was implemented in three areas (the Salla and Kittilä lobes and Sodankylä interlobate complex) based on the analysis of digital elevation model (DEM) and a geological mapping dataset.

- Flow direction analysis suggests a northern location for the ice-divide zone during the Early/Middle Weichselian, and a more W/SW position for the Late Weichselian.
- A distinct NNW orientation of the lineations is visible both in Kittilä and in Salla, whereas in the Sodankylä area, the streamlined features show a more diverse pattern.
- The current topography reflects pre Late Weichselian glacial flow directions rather than those of the Late Weichselian

The results obtained in this study indicate that groundwater flow modeling should be based on a solid 3D understanding of the geological features of the modeled area, especially in hydrostratigraphically heterogenic environments.

- Complex geological 3D models are essential for groundwater flow modelling if complex recharge and discharge patterns are observed or if high variation of hydraulic conductivity is present. Complex hydrostratigaphical models generated more complicated recharge and discharge patterns, whereas in simple models, the modelled groundwater flow was more horizontal.
- Interlayered low conductivity units should be taken into account in 3D hydrostratigraphical models since they refract flow lines affecting to the locations of groundwater recharge and discharge areas.

References

Aalto, M., Eriksson, B. & Hirvas, H. 1992. Naakenavaara interglacial; a till-covered peat deposit in western Finnish Lapland. Bulletin of the Geological Society of Finland 64, 169–181.

Åberg, S.C, Korkka-Niemi, K., Rautio, A.B.K. & Åberg, A.K. The effect of river regulation on groundwater flow patterns and the hydrological conditions of an aapa mire in northern Finland. In prep.

Åberg, S.C, Korkka-Niemi, K., Rautio, A.B.K., Salonen, V.-P. & Åberg, A.K. 2019. Groundwater recharge/discharge patterns and groundwater–surface water interactions in a sedimentary aquifer along the River Kitinen in Sodankylä. Boreal Environment Research 24, 155–187.

Aitken, M.J. 1985. Thermoluminescence dating. Studies on Archaeological Science. Academic Press Inc., London, 359 p.

Allen, D.M., Schuurman, N., Deshpande, A. & Scibek, J. 2008. Data integration and standardization in cross-border hydrogeological studies: a novel approach to hydrostratigraphic model development. Environmental Geology 53, 1441–1453. https://doi.org/10.1007/s00254-007-0753-3

Anand, R.R. & Paine M. 2002. Regolith geology of the Yilgarn Craton, Western Australia: implications for exploration. Australian Journal of Earth Sci-

ences 49, 3–162. https://doi.org/10.1046/j.1440-0952.2002.00912.x

Andersen, K.K., Svensson, A., Johnsen, S.J., Rasmussen, S.O., Bigler, M., Röthlisberger, R., Ruth, U., Siggaard-Andersen, M.-L., Peder Steffensen, J., Dahl-Jensen, D., Vinther, B.M. & Clausen, H.B. 2006. The Greenland Ice Core Chronology 2005, 15–42ka. Part 1: constructing the time scale. Quaternary Science Reviews 25, 3246–3257. https://doi.org/10.1016/j.quascirev.2006.08.002

Artimo, A., Salonen, V.-P., Pietilä, S. & Saraperä, S. 2004. Three-dimensional geologic modeling and groundwater flow modeling of the Töllinperä Aquifer in the Hitura nickel mine area, Finland; providing the framework for restoration and protection of the aquifer. Bulletin of the Geological Society of Finland 76, 5–17. https://doi.org/10.17741/BGSF/76.1-2.001

Auri, J., Breilin, O., Hirvas, H., Huhta, P., Johansson, P., Mäkinen, K., Nenonen, K. & Sarala, P. 2008. Tiedonanto eräiden myöhäispleistoseenikerrostumien avainkohteiden ajoittamisesta Suomessa. Geologi 60, 68–74.

Batchelor, C.L., Margold, M., Krapp, M., Murton, D.K., Dalton, A.S., Gibbard, P.L., Stokes, C.R., Murton, J.B. & Manica, A. 2019. The configuration of Northern Hemisphere ice sheets through the Quaternary. Nature Communications 10, 3713. https://doi.org/10.1038/s41467-019-11601-2

Behre, K.-E. & Lade, U. 1986. Eine Folge von Eem und 4 Weichsel-Interstadialen in Oerel/Niedersachsen und ihr Vegetationsablauf. Eiszeiten und Gegenwart 36, 11–36. https://doi.org/10.3285/eg.36.1.02

Berger, A. & Loutre M.F. 1991. Insolation values for the climate of the last 10 million years. Quaternary Science Reviews 10, 297–317. https://doi.org/10.1016/0277-3791(91)90033-Q

Bøtter-Jensen, L. & Duller, G.A.T. 1992. A new system for measuring optically stimulated luminescence from Quaternary samples. International Journal of Radiation Applications and Instrumentation. Part D. Nuclear Tracks and Radiation Measurements 20, 549–553. https://doi.org/10.1016/1359-0189(92)90003-E

Bøtter-Jensen, L., Duller, G.A.T., Murray, A. & Banerjee, D. 1999. Blue Light Emitting Diodes for Optical Stimulation of Quartz in Retrospective Dosimetry and Dating. Radiation Protection Dosimetry 84, 335–340 https://doi.org/10.1093/oxfordjournals.rpd.a032750

Bøtter-Jensen, L. & Mejdahl, V. 1988. Assessment of beta dose-rate using a GM multicounter system. International Journal of Radiation Applications and Instrumentation. Part D. Nuclear Tracks and Radiation Measurements 14, 187–191. https://doi.org/10.1016/1359-0189(88)90062-3

Brownscombe, W., Ihlenfeld, C., Coppard, J., Hartshorne, C., Klatt, S., Siikaluoma, J.K. & Herrington, R.J. 2015. Chapter 3.7 - The Sakatti Cu-Ni-PGE Sulfide Deposit in Northern Finland. In: Maier, W.D., Lahtinen, R., O'Brien, H. (eds.), Mineral Deposits of Finland, Elsevier, Amsterdam, pp. 211–252. https://doi.org/10.1016/B978-0-12-410438-9.00009-1

Cutler, K.B., Edwards, R.L., Taylor, F.W., Cheng, H., Adkins, J., Gallup, C.D., Cutler, P.M., Burr, G.S. & Bloom, A.L. 2003. Rapid sea-level fall and deep-ocean temperature change since the last interglacial period. Earth and Planetary Science Letters 206, 253–271. https://doi.org/10.1016/S0012-821X(02)01107-X

Dansgaard, W., Johnsen, S.J., Clausen, H.B., Dahl-Jensen, D., Gundestrup, N.S., Hammer, C.U., Hvidberg, C.S., Steffensen, J.P., Sveinbjörnsdottir, A.E., Jouzel, J. & Bond, G. 1993. Evidence for general instability of past climate from a 250-kyr ice-core record. Nature 364, 218–220. https://doi.org/10.1038/364218a0

Ebert, K., Hall, A.M., Kleman, J. & Andersson, J. 2015. Unequal ice-sheet erosional impacts across low-relief shield terrain in northern Fennoscandia. Geomorphology 233, 64–74. https://doi.org/10.1016/j.geomorph.2014.09.024

Eilu, P. 2012. (ed) Mineral deposits and metallogeny of Fennoscandia. Geological Survey of Finland, Special paper 53, Espoo, Finland, 403 p.

Emiliani, C. 1961. Cenozoic Climatic Changes as Indicated by the Stratigraphy and Chronology of Deep-Sea Cores of Globigerina-Ooze Facies. Annals of the New York Academy of Sciences 95, 521–536. https://doi.org/10.1111/j.1749-6632.1961.tb50057.x

Eyles, N., Eyles, C.H. & Miall, A.D. 1983. Lithofacies types and vertical profile models; an alternative approach to the description and environmental interpretation of glacial diamict and diamictite sequences. Sedimentology 30, 393–410. https://doi.org/10.1111/j.1365-3091.1983.tb00679.x

Freeze, R.A. & Witherspoon, P.A. 1967. Theoretical analysis of regional groundwater flow: 2. Effect of water-table configuration and subsurface permeability variation. Water Resources Research 3, 623–634.

Giaccio, B., Nomade, S., Wulf, S., Isaia, R., Sottili, G., Cavuoto, G., Galli, P., Messina, P., Sposato, A., Sulpizio, R. & Zanchetta, G. 2012. The late MIS 5 Mediterranean tephra markers: a reappraisal from peninsular Italy terrestrial records. Quaternary Science Reviews 56, 31–45. https://doi.org/10.1016/j.quascirev.2012.09.009

Gray, N.F. 1997. Environmental impact and remediation of acid mine drainage: a management problem. Environmental Geology 30, 62–71. https://doi.org/10.1007/s002540050133

Greenwood, S.L., Clason, C.C., Helanow, C. & Margold, M. 2016. Theoretical, contemporary observational and palaeo-perspectives on ice sheet hy-

drology: Processes and products. Earth-Science Reviews 155, 1–27. https://doi.org/10.1016/j.earscirev.2016.01.010

GTK 2018. Bedrock of Finland (scale free). Digital Map. https://hakku.gtk.fi/locations/search?location_id=181 (visited 7/2019)

Gustavsson, N., Noras, P. & Tanskanen, H. 1979. Seloste geokemiallisen kartoituksen tutkimusmenetelmistä. Geologinen tutkimuslaitos, Espoo, 20 p.

Hall, A.M., Sarala, P. & Ebert, K. 2015. Late Cenozoic deep weathering patterns on the Fennoscandian shield in northern Finland: A window on ice sheet bed conditions at the onset of Northern Hemisphere glaciation. Geomorphology 246, 472–488. http://dx.doi.org/10.1016/j.geomorph.2015.06.037

Hanski, E. & Huhma, H. 2005. Central Lapland greenstone belt. In: Lehtinen, M., Nurmi, P. & Rämö, T. (eds.), Precambrian Geology of Finland, Elsevier, Amsterdam, pp. 139–193. https://doi.org/10.1016/S0166-2635(05)80005-2

Hanski, E., Huhma, H. & Vaasjoki, M. 2001. Geochronology of northern Finland: a summary and discussion. Geological Survey of Finland, Special Paper 33, 255–279.

Hättestrand, M. & Robertsson, A.-M. 2010. Weichselian interstadials at Riipiharju, northern Sweden – interpretation of vegetation and climate from fossil and modern pollen records. Boreas 39, 296–311. https://doi.org/10.1111/j.1502-3885.2009.00129.x

Hättestrand, C. & Stroeven, A.P. 2002. A relict landscape in the centre of Fennoscandian glaciation: Geomorphological evidence of minimal Quaternary glacial erosion. Geomorphology 44, 127–143. https://doi.org/10.1016/S0169-555X(01)00149-0

Heikkinen, A., Koivisto, A. K. & Äikää, O. 1974. Geological Survey of Finland, Radiocarbon measurements VI. Radiocarbon 16, 252–268.

Helmens, K.F. 2014. The Last Interglacial–Glacial cycle (MIS 5–2) re-examined based on long proxy records from central and northern Europe. Quaternary Science Reviews 86, 115–143. https://doi.org/10.1016/j.quascirev.2013.12.012

Helmens, K.F., Bos, J.A.A., Engels, S., Van Meerbeeck, C.J., Bohncke, S.J.P., Renssen, H., Heiri, O., Brooks, S.J., Seppä, H. & Wohlfarth, B. 2007a. Present-day temperatures in northern Scandinavia during the last glaciation. Geology 35, 987–990. https://doi.org/10.1130/G23995A.1

Helmens, K.F., Johansson, P.W., Räsänen, M., Alexanderson, H. & Eskola, K.O. 2007b. Ice-free intervals continuing into Marine Isotope Stage 3 at Sokli in the central area of the Fennoscandian glaciations. Bulletin of the Geological Society of Finland 79, 17–39.

Helmens, K.F., Katrantsiotis, C., Salonen, S.J., Shala, S., Bos, J.A.A., Engels, S., Kuosmanen, N., Luoto, T.P., Väliranta, M., Luoto, M., Ojala, A., Risberg, J. & Weckström, J. 2018. Warm summers and rich biotic communities during N-Hemisphere deglaciation. Global and Planetary Change 167, 61–73. https://doi.org/10.1016/j.gloplacha.2018.05.004

Helmens, K.F., Räsänen, M.E., Johansson, P.W., Jungner, H. & Korjonen, K. 2000. The Last Interglacial-Glacial cycle in NE Fennoscandia: a nearly continuous record from Sokli (Finnish Lapland). Quaternary Science Reviews 19, 1605–1623. https://doi.org/10.1016/S0277-3791(00)00004-4

Helmens, K.F., Risberg, J., Jansson, K.N., Weckström, J., Berntsson, A., Tillman, P.K., Johansson, P.W. & Wastegård, S. 2009. Early MIS 3 glacial lake evolution, ice-marginal retreat pattern and climate at Sokli (northeastern Fennoscandia). Quaternary Science Reviews 28, 1880–1894. https://doi.org/10.1016/j.quascirev.2009.03.001

Hirvas, H. 1991. Pleistocene stratigraphy of Finnish Lapland. Geological Survey of Finland, Bulletin 354, 123 p.

Hirvas, H., Alfthan, A., Pulkkinen, E., Puranen, R. & Tynni, R. 1977. Raportti malminetsintää palvelevasta maaperätutkimuksesta Pohjois-Suomessa vuosina 1972–1976. Geological Survey of Finland 19, 54 p.

Hirvas, H., Saarnisto, M., Hakala, P., Huhta, P., Johansson, P. & Pulkkinen, E. 1994. Maaperän kerrosjärjestys ja geokemia Keivitsassa. Geological Survey of Finland, Report number 4320, 44 p.

Hjelt, A. & Pääkkö, E. 2006. Viiankiaavan hoito- ja käyttösuunnitelma. Metsähallituksen luonnonsuojelujulkaisuja, Sarja C 11, Metsähallitus, Vantaa, 51 p.

Howett, P.J., Salonen, V.-P., Hyttinen, O., Korkka-Niemi, K. & Moreau, J. 2015. A hydrostratigraphical approach to support environmentally safe siting of a mining waste facility at Rautuvaara, Finland. Bulletin of the Geological Society of Finland 87, 51–66. http://dx.doi.org/10.17741/bgsf/87.2.001

Hudon-Gagnon, E., Chesnaux, R., Cousineau, P.A. & Rouleau A. 2015. A hydrostratigraphic simplification approach to build 3D groundwater flow numerical models: example of a Quaternary deltaic deposit aquifer. Environmental Earth Sciences, 74, 4671–468. https://doi.org/10.1007/s12665-015-4439-y

Hughes, A.L.C., Gyllencreutz, R., Lohne, Ø.S., Mangerud, J. & Svendsen, J.I. 2016. The last Eurasian ice sheets – a chronological database and time-slice reconstruction, DATED-1. Boreas 45, 1–45. https://doi.org/10.1111/bor.12142

Hyyppä, J. 1977. Kaoliinia Sodankylän Siurunmaassa. Geologi 29, 52–56.

Hyyppä, J. 1983. Suomen kallioperän preglasiaalisesta rapautumisesta. In: Pokki E. (ed.), Rapautuminen kallioperässä. Symposium 9.11.1983, Rakennusgeologinen yhdistys, Espoo, pp. II/1–18.

Johansson, P. 1995. The deglaciation in the eastern part of the Weichselian ice divide in Finnish Lapland.

Geological Survey of Finland, Bulletin 383, 72 p.
Johansson, P. & Kujansuu, R. 2005. Pohjois-Suomen maaperä: maaperäkarttojen 1:400 000 selitys. Geologian tutkimuskeskus (GTK), Espoo, 236 p.
Johansson, P., Lunkka, J.P. & Sarala, P. 2011. The glaciation of Finland. In: Ehlers J., Gibbard P.L. & Hughes P.D. (eds.), Quaternary Glaciations – Extent and Chronology, A closer look, Developments in Quaternary Science 15, Elsevier, Amsterdam, pp. 105–116.
Johnsen, S.J., Clausen, H.B., Dansgaard, W., Fuhrer, K., Gundestrup, N., Hammer, C.U., Iversen, P., Jouzel, J., Stauffer, B. & Steffensen, J.P. 1992. Irregular glacial interstadials recorded in a new Greenland ice core. Nature 359, 311–313. https://doi.org/10.1038/359311a0
Jungner, H. 1979. Radiocarbon dates I. Dating Laboratory, University of Helsinki, Finland, Report no. 1, 77 p.
Jungner, H. & Sonninen, E. 1983. Radiocarbon dates II. Radiocarbon Dating Laboratory, University of Helsinki, Report No 2, 121 p.
Kauppi, S., Mannio, J., Hellsten, S., Nystén, T., Jouttijärvi, T., Huttunen, M., Ekholm, P., Tuominen, S. Porvari, P., Karjalainen, A., Sara-Aho, T., Saukkoriipi, J. & Maunula, M. 2013. Arvio Talvivaarankaivoksen kipsisakka-altaan vuodon haitoista ja riskeistä vesiympäristölle. Suomen ympäristökeskuksen raportteja 11/2013, 90 p.
Kleman, J., Hättestrand, C., Borgström, I. & Stroeven, A. 1997. Fennoscandian palaeoglaciology reconstructed using a glacial geological inversion model. Journal of Glaciology 43, 283–299. https://doi.org/10.3189/S0022143000003233
Kujansuu, R. 1967. On the deglaciation of western Finnish Lapland. Bulletin de la Commission Geologique de Finlande 232, 98 p.
Kupila, J., Davidila, J., Lintinen, P., Valpola, S., Rossi, P., Sanaksenaho, R. & Lindholm, A. 2020. Pohjavesien suojelun ja kiviaineshuollon yhteensovittaminen Lapissa, vaihe 2 (Lapin Poski2), 76 p., 7 appendices.
Lappalainen, E. 2004. Kallio - ja maaperä sekä kasvillisuuden jääkauden jälkeinen kehityshistoria. In Pääkkö, E. (ed.) 2004. Keski-Lapin aapasoiden luonto (eng. Ecological surveys of aapa mires in Central Lapland). Metsähallituksen luonnonsuojelujulkaisuja. Sarja A 145, Vantaa, pp. 18–45.
Lappalainen, E. 1970. Über die spätquartäre Entwicklung der Flussufermoore Mittel-Lapplands. Bulletin de la Commission Geologique de Finlande 244, 79 p.
Lappalainen, E. & Pajunen, H. 1980. Lapin turvevarat: yhteenveto vuosina 1962–1975 Lapissa tehdyistä turvetutkimuksista. Geologinen tutkimuslaitos, Espoo, 229 p.
Leskelä, S. 1971. Auger-kairaus Sodankylässä 5.7–24.7.1971. Geological Survey of Finland, Report number 1413, 7 p., 2 maps.
Lestinen, P., 1980. The results of the geochemical survey in the Peurasuvanto map-sheet area (in Finnish with English summary). Geological Survey of Finland 3723, 97.
Lisiecki, L.E. & Raymo, M.E. 2005. A Pliocene-Pleistocene stack of 57 globally distributed benthic $\delta^{18}O$ records. Paleoceanography 20. https://doi.org/10.1029/2004PA001071
Lundqvist, J. 1986. Late Weichselian glaciation and deglaciation in Scandinavia. Quaternary Science Reviews 5, 269–292. https://doi.org/10.1016/0277-3791(86)90192-7
Lundqvist, J. & Wohlfarth, B. 2000. Timing and east–west correlation of south Swedish ice marginal lines during the Late Weichselian. Quaternary Science Reviews 20, 1127–1148. https://doi.org/10.1016/S0277-3791(00)00142-6
Lunkka, J.P., Sarala, P. & Gibbard, P.L. 2015. The Rautuvaara section, western Finnish Lapland, revisited: new age constraints indicate a complex Scandinavian Ice Sheet history in northern Fennoscandia during the Weichselian Stage. Boreas 44, 68–80. https://doi.org/10.1111/bor.12088
Mäkilä, M., Säävuori, H., Kuznetsov, O. & Grundström, A. 2013. Age and dynamics of peatlands in Finland. Geological Survey of Finland, Report of Peat Investigation 443, 41 p.
Martinson, D.G., Pisias, N.G., Hays, J.D., Imbrie, J., Moore, T.C. & Shackleton, N.J. 1987. Age dating and the orbital theory of the ice ages: Development of a high-resolution 0 to 300,000-year chronostratigraphy. Quaternary Research 27, 1–29. https://doi.org/10.1016/0033-5894(87)90046-9
Murray, A.S. & Wintle, A.G. 2000. Luminescence dating of quartz using an improved single-aliquot regenerative-dose protocol. Radiation Measurements, 32, 57–73. https://doi.org/10.1016/S1350-4487(99)00253-X
Neal, A. 2004. Ground-penetrating radar and its use in sedimentology: principles, problems and progress. Earth-Science Reviews 66, 261–330. https://doi.org/10.1016/j.earscirev.2004.01.004
Nenonen, K. 1995. Pleistocene stratigraphy and reference sections in southern and western Finland. Academic Dissertation, Geological Survey of Finland, 94 p.
Niiranen, T., Lahti, I. & Nykänen, V. 2015. Chapter 10.2 - The Orogenic Gold Potential of the Central Lapland Greenstone Belt, Northern Fennoscandian Shield. In: Maier, W.D., Lahtinen, R. & O'Brien, H. (eds.), Mineral Deposits of Finland, Elsevier, pp. 733–752. https://doi.org/10.1016/B978-0-12-410438-9.00028-5
Niiranen, T., Poutiainen, M. & Mänttäri, I. 2007. Geology, geochemistry, fluid inclusion characteristics, and U–Pb age studies on iron oxide–Cu–Au deposits in the Kolari region, northern Finland. Ore Geology Reviews 30, 75–105. https://doi.org/10.1016/j.oregeorev.2005.11.002

North Greenland Ice-Core Project members, Andersen, K.K., Azuma, N., Barnola, J.M., Bigler, M., Biscaye, P., Caillon, N., Chappellaz, J., Clausen, H.B., Dahl-Jensen, D., Fischer, H., Flückiger, J., Fritzsche, D., Fujii, Y., Goto-Azuma, K., Grønvold, K., Gundestrup, N.S., Hansson, M., Huber, C., Hvidberg, C.S., Johnsen, S.J., Jonsell, U., Jouzel, J., Kipfstuhl, S., Landais, A., Leuenberger, M., Lorrain, R., Masson-Delmotte, V., Miller, H., Motoyama, H., Narita, H., Popp, T., Rasmussen, S.O., Raynaud, D., Röthlisberger, R., Ruth, U., Samyn, D., Schwander, J., Shoji, H., Siggard-Andersen, M.L., Steffensen, J.P., Stocker, T., Sveinbjörnsdottir, A.E., Svensson, A., Takata, M., Tison, J.L., Thorsteinsson, T., Watanabe, O., Wilhelms, F. & White, J. 2004. High-resolution record of the Northern Hemisphere climate extending into the last interglacial period. Nature, 431, 147–151.

Nydahl, R., Gulliksen, S. & Lövseth, K., 1972. Trondheim natural radiocarbon measurements VI. Radiocarbon 14, 418–451. https://doi.org/10.1017/S0033822200059476

Obrochta, S.P., Yokoyama, Y., Morén, J. & Crowley, T.J. 2014. Conversion of GISP2-based sediment core age models to the GICC05 extended chronology. Quaternary Geochronology 20, 1–7. https://doi.org/10.1016/j.quageo.2013.09.001

Olsen, L., Mejdahl, V. & Selvik, S.F. 1996. Middle and Late Pleistocene stratigraphy, chronology and glacial history in Finnmark, North Norway. Norges geologiske undersøkelse Bulletin 429, 1–111.

Pääkkö, E. 2004. Keski-Lapin aapasoiden luonto, Metsähallituksen luonnonsuojelujulkaisuja. Sarja A, 145, 153 p.

Parker, A. 1970. An index of weathering for silicate rocks. Geological Magazine 107, 501–550. https://doi.org/10.1017/S0016756800058581

Patton H., Hubbard A., Andreassen K., Auriac A., Whitehouse P.L., Stroeven A.P., Shackleton C., Winsborrow M., Heyman J. & Hall A.M. 2017. Deglaciation of the Eurasian ice sheet complex. Quaternary Science Reviews 169, 148–172. https://doi.org/10.1016/j.quascirev.2017.05.019

Patton, H., Hubbard, A., Andreassen, K., Winsborrow, M. & Stroeven, A.P. 2016. The build-up, configuration, and dynamical sensitivity of the Eurasian ice-sheet complex to Late Weichselian climatic and oceanic forcing. Quaternary Science Reviews 153, 97–121. https://doi.org/10.1016/j.quascirev.2016.10.009

Penttilä, S. 1963. The deglaciation of the Laanila area, Finnish Lapland. Bulletin de la Commission Geologique de Finlande 203, 71 p., 1 map.

Peuraniemi, V., Aario, R. & Pulkkinen, P. 1997. Mineralogy and geochemistry of the clay fraction of till in northern Finland. Sedimentary Geology 111, 313–327. https://doi.org/10.1016/S0037-0738(97)00023-7

Pitkäranta, R. 2009. Lithostratigraphy and age estimations of the Pleistocene erosional remnants near the centre of the Scandinavian glaciations in western Finland. Quaternary Science Reviews 28, 166–180. https://doi.org/10.1016/j.quascirev.2008.10.003

Pulkkinen, E. 1983. Sattasen karttalehtialueen geokemiallisen kartoituksen tulokset. Geological Survey of Finland, Espoo, 67 p.

Punkari, M. 1997. Glacial and glaciofluvial deposits in the interlobate areas of the Scandinavian Ice Sheet. Quaternary Science Reviews 16, 741–753.

Putkinen, N., Eyles, N., Putkinen, S., Ojala, A.E., Palmu, J.-P., Sarala, P., Väänänen, T., Räisänen, J., Saarelainen, J., Ahtonen, N., Rönty, H., Kiiskinen, A., Rauhaniemi, T. & Tervo, T. 2017. High-resolution LiDAR mapping of glacial landforms and ice stream lobes in Finland. Bulletin of the Geological Society of Finland 89, 64–81. https://doi.org/10.1016/j.qsa.2020.100005

Putkinen, N., Sarala, P., Eyles, N., Daxberger, H., Pihlaja, J. & Murray, A. 2020. Reworked Middle Pleistocene deposits preserved in the core region of the Fennoscandian Ice Sheet. Quaternary Science Advances 2, 100005.

Raatikainen, M. 2019. Moreenin hienoaineksen koostumukseen vaikuttavat tekijät Keski-Lapin alueella. Bachelor's thesis, University of Oulu, 25 p.

Rainio, H., Saarnisto, M. & Ekman, I. 1995. Younger Dryas end moraines in Finland and NW Russia. Quaternary international 28, 179–192. https://doi.org/10.1016/1040-6182(95)00051-J

Räisänen, J. 2014. Sodankylän alueen maaperäkartoitus 2013-2014 (Väliraportti). GTK:n arkistoraportit, Geologian tutkimuskeskus, Rovaniemi, 22 p.

Ramboll 2020. Liite 6: Sakatin monimetalliesiintymän kaivoshankkeen vaikutukset Viiankiaavan Natura 2000 -alueeseen.

Räsänen, M.E., Huitti, J.V., Bhattarai, S., Harvey, J. & Huttunen, S. 2015. The SE sector of the Middle Weichselian Eurasian Ice Sheet was much smaller than assumed. Quaternary Science Reviews 122, 131–141. https://doi.org/10.1016/j.quascirev.2015.05.019

Rask, M. & Lintinen, P. 2001. Kaoliinitutkimukset Sodankylän Siurunmaalla vuosina 1978–1988. Geological Survey of Finland, 12 p., 6 appendices.

Rasmussen, S.O., Andersen, K.K., Svensson, A.M., Steffensen, J.P., Vinther, B.M., Clausen, H.B., Siggaard-Andersen, M.-L., Johnsen, S.J., Larsen, L.B., Dahl-Jensen, D., Bigler, M., Röthlisberger, R., Fischer, H., Goto-Azuma, K., Hansson, M.E. & Ruth, U. 2006. A new Greenland ice core chronology for the last glacial termination. Journal of Geophysical Research 111. https://doi.org/10.1029/2005JD006079

Rasmussen, S.O., Bigler, M., Blockley, S.P., Blunier, T., Buchardt, S.L., Clausen, H.B., Cvijanovic, I., Dahl-Jensen, D., Johnsen, S.J., Fischer, H., Gkinis,

V., Guillevic, M., Hoek, W.Z., Lowe, J.J., Pedro, J.B., Popp, T., Seierstad, I.K., Steffensen, J.P., Svensson, A.M., Vallelonga, P., Vinther, B.M., Walker, M.J.C., Wheatley, J.J. & Winstrup, M. 2014. A stratigraphic framework for abrupt climatic changes during the Last Glacial period based on three synchronized Greenland ice-core records: refining and extending the INTIMATE event stratigraphy. Quaternary Science Reviews 106, 14–28. https://doi.org/10.1016/j.quascirev.2014.09.007

Rasmussen, S.O., Seierstad, I.K., Andersen, K.K., Bigler, M., Dahl-Jensen, D. & Johnsen, S.J. 2008. Synchronization of the NGRIP, GRIP, and GISP2 ice cores across MIS 2 and palaeoclimatic implications. Quaternary Science Reviews 27, 18–28. https://doi.org/10.1016/j.quascirev.2007.01.016

Rautio, A.B., Korkka-Niemi, K.I. & Salonen, V.-P. 2018. Thermal infrared remote sensing in assessing groundwater and surface-water resources related to Hannukainen mining development site, northern Finland. Hydrogeoly Journal 26, 163–183. https://doi.org/10.1007/s10040-017-1630-0

Rossi, S. 1991. Rapakallion kuparianomalian malmitutkimukset Maaselässä Sodankylän kunnan pohjoisosassa vuosina 1977–1983. Geological Survey of Finland, 48 p., 8 appendices.

Salmi, M. 1965. Sodankylän Sattasen glasiaaligeologiasta. M.Sc. Thesis, University of Oulu, Finland, 57 p., 2 appendices

Salminen, R. 1972. Auger-kairaus Sodankylässä keväällä 1972. Geological Survey of Finland, 7 p., 24 appendices.

Salonen, V.-P. 2019. Viiankiaavan ympäristön maaperän kehitys ja sen erityispiirteet. Summary: Quaternary history and sediments around the Sakatti deposit, Sodankylä. Raportti 23.5. 2019. AA Sakatti Mining Oy/Salonen Environment, 43 p.

Salonen, V.-P., Kaakinen, A., Kultti, S., Miettinen, A., Eskola, K. & Lunkka, J. 2008. Middle Weichselian glacial event in the central part of the Scandinavian Ice Sheet recorded in the Hitura pit, Ostrobothnia, Finland. Boreas 37, 38–54. https://doi.org/10.1111/j.1502-3885.2007.00009.x

Salonen, V.-P., Korkka-Niemi K., Moreau, J. & Rautio, A. 2014a. Kaivokset ja vesi: esimerkkinä Hannukaisen hanke. Geologi 66, 8–19.

Salonen, V.-P., Moreau, J., Hyttinen, O. & Eskola, K.O. 2014b. Mid-Weichselian interstadial in Kolari, western Finnish Lapland. Boreas 43, 627–638. https://doi.org/10.1111/bor.12060

Sarala, P. 2005. Weichselian stratigraphy, geomorphology and glacial dynamics in southern Finnish Lapland. Bulletin of the Geological Society of Finland 77, 71–103.

Sarala, P., Räisänen, J., Johansson, P. & Eskola, K.O. 2015. Aerial LiDAR analysis in geomorphological mapping and geochronological determination of surficial deposits in the Sodankylä region, northern Finland. GFF 137, 293–303. https://doi.org/10.1080/11035897.2015.1100213

Shackleton, N.J. 1969. The last interglacial in the marine and terrestrial records. Proceedings of the Royal Society of London. Series B. Biological Sciences 174, 135–154. https://doi.org/10.1098/rspb.1969.0085

Shackleton, N.J. 1987. Oxygen isotopes, ice volume and sea level. Quaternary Science Reviews 6, 183–190. https://doi.org/10.1016/0277-3791(87)90003-5

Siegert, M.J., Dowdeswell, J.A., Hald, M. & Svendsen, J.-I. 2001. Modelling the Eurasian Ice Sheet through a full (Weichselian) glacial cycle. Global and Planetary Change 31, 367–385. https://doi.org/10.1016/S0921-8181(01)00130-8

Siivonen, L. 1975. New results on the history and taxonomy of the mountain, forest and domestic reindeer in Northern Europe. Proceedings of the First International Reindeer and Caribou Symposium, Fairbanks 1972. Biological Papers of the University of Alaska, Special Report 1, 33–41.

Stroeven, A.P., Hättestrand, C., Kleman, J., Heyman, J., Fabel, D., Fredin, O., Goodfellow, B.W., Harbor, J.M., Jansen, J.D., Olsen, L., Caffee, M.W., Fink, D., Lundqvist, J., Rosqvist, G.C., Strömberg, B. & Jansson, K.N. 2016. Deglaciation of Fennoscandia. Quaternary Science Reviews 147, 91–121. https://doi.org/10.1016/j.quascirev.2015.09.016

Sun, Q., Shao, J., Wang, Y. & Ma, T. 2019. Research on appropriate borehole density for establishing reliable geological model based on quantitative uncertainty analysis. Arabian Journal of Geosciences 12, 410. https://doi.org/10.1007/s12517-019-4533-7

Suonperä, E. 2016. Holocene paleohydrology of Viiankiaapa mire, Sodankylä, Finnish Lapland. MSc Thesis, University of Helsinki, Helsinki, 81 p., 5 appendices.

Sutinen, R. 1992. Glacial deposits, their electrical properties and surveying by image interpretation and ground penetrating radar. Geological Survey of Finland, Bulletin 359, 123 p.

Svendsen, J.I., Alexanderson, H., Astakhov, V.I., Demidov, I., Dowdeswell, J.A., Funder, S., Gataullin, V., Henriksen, M., Hjort, C., Houmark-Nielsen, M., Hubberten, H.W., Ingólfsson, Ó., Jakobsson, M., Kjær, K.H., Larsen, E., Lokrantz, H., Lunkka, J.P., Lysså, A., Mangerud, J., Matiouchkov, A., Murray, A., Möller, P., Niessen, F., Nikolskaya, O., Polyak, L., Saarnisto, M., Siegert, C., Siegert, M.J., Spielhagen, R.F. & Stein, R. 2004. Late Quaternary ice sheet history of northern Eurasia. Quaternary Science Reviews 23, 1229–1271. https://doi.org/10.1016/j.quascirev.2003.12.008

Svensson, A., Andersen, K.K., Bigler, M., Clausen, H.B., Dahl-Jensen, D., Davies, S.M., Johnsen,

S.J., Muscheler, R., Rasmussen, S.O., Röthlisberger, R., Peder Steffensen, J. & Vinther, B.M. 2006. The Greenland Ice Core Chronology 2005, 15–42ka. Part 2: comparison to other records. Quaternary Science Reviews 25, 3258–3267. https://doi.org/10.1016/j.quascirev.2006.08.003

Tanner, V. 1915. Studier öfver kvartärsystemet i Fennoskandias nordliga delar. III. Om landisens rörelsor och afsmälting i finska Lappland och angränsande trakter. Bulletin de la Commission Géologique de Finlande 38, 815 p.

Tanner, V. 1930. Studier över kvartärsystemet i Fennoskandias nordliga delar IV. Om nivaförändringarna och grunddragen av den geografiska utvecklingen efter istiden i Ishavsfinland samt om homotaxin av fennoskandias kvartära marina avlagringar Bulletin de la Commission Géologique de Finlande 88, 589 p.

Tie- ja vesirakennushallitus 1973. Maarakennusalan tutkimus-ja suunnitteluohjeita, osa II. Valtionpainatuskeskus, Helsinki, 153 p.

Tyrväinen, A. 1980. Suomen geologinen kartta 1:100 000: Lehti = Sheet 3714. Sattanen kallioperäkartta = Geological map of Finland 1:100 000; Pre-Quaternary rocks. Geological Survey of Finland.

Tyrväinen, A. 1983. Suomen geologinen kartta 1:100 000: Lehdet = Sheets 3713 ja 3714. Sodankylän ja Sattasen kartta-alueiden kallioperä = Pre-Quaternary rocks of the Sodankylä and Sattanen map-sheet areas kallioperäkarttojen selitykset = Geological map of Finland 1:100 000; explanation to the maps of pre-Quaternary rocks. Geological Survey of Finland, Espoo, 59 p.

Ukkonen, P., Arppe, L., Houmark-Nielsen, M., Kjær, K.H. & Karhu, J.A. 2007. MIS 3 mammoth remains from Sweden—implications for faunal history, palaeoclimate and glaciation chronology. Quaternary Science Reviews 26, 3081–3098. https://doi.org/10.1016/j.quascirev.2007.06.021

Ukkonen, P., Lunkka, J.P., Jungner, H. & Donner, J. 1999. New radiocarbon dates from Finnish mammoths indicating large ice-free areas in Fennoscandia during the Middle Weichselian. Journal of Quaternary science 14, 711–714. https://doi.org/10.1002/(SICI)1099-1417(199912)14:7<711::AID-JQS506>3.0.CO;2-E

Virkkala, K. 1955. On the glacifluvial erosion and accumulation in Tankavaara area, Finnish Lapland. Acta Geografica 14, 393–412.

Woillard, G.M. 1978. Grande Pile peat bog: a continuous pollen record for the last 140000 years. Quaternary Research 9, 1–21. https://doi.org/10.1016/0033-5894(78)90079-0